

Copyright Warning & Restrictions

The copyright law of the United States (Title 17, United States Code) governs the making of photocopies or other reproductions of copyrighted material.

Under certain conditions specified in the law, libraries and archives are authorized to furnish a photocopy or other reproduction. One of these specified conditions is that the photocopy or reproduction is not to be “used for any purpose other than private study, scholarship, or research.” If a user makes a request for, or later uses, a photocopy or reproduction for purposes in excess of “fair use” that user may be liable for copyright infringement,

This institution reserves the right to refuse to accept a copying order if, in its judgment, fulfillment of the order would involve violation of copyright law.

Please Note: The author retains the copyright while the New Jersey Institute of Technology reserves the right to distribute this thesis or dissertation

Printing note: If you do not wish to print this page, then select “Pages from: first page # to: last page #” on the print dialog screen

The Van Houten library has removed some of the personal information and all signatures from the approval page and biographical sketches of theses and dissertations in order to protect the identity of NJIT graduates and faculty.

ABSTRACT

LOW FREQUENCY CHARACTERIZATION OF A LOOP ANTENNA

by
Irene Koukhta

The conventional solution of an integral equation for the loop antenna in free space can be expressed analytically using Fourier Series. However, the solutions based on delta gap feed model yield divergent input susceptance.

To overcome such diverging results, alternative solution using equivalent magnetic frill current feed models were implemented. Although low frequency models for delta gap feeds were suggested, no generalized low frequency expansions for the input admittance have been reported previously. In this work, such generalized low frequency expansion are developed for both delta-gap and magnetic frill feeds of loop antennas. Validity of such expansion have been investigated comparing them with the published results.

One other advantage of keeping such expansions limited to only few terms is to associate each term with the equivalent inductance, resistance, capacitance, radiation conductance and susceptance of the antenna.

Blank Page

LOW FREQUENCY CHARACTERIZATION OF A LOOP ANTENNA

by
Irene Koukhta

**A Thesis
Submitted to the Faculty of
New Jersey Institute of Technology
in Partial Fulfillment of Requirements for the Degree of
Master of Science in Electrical Engineering**

Department of Electrical and Computer Engineering

May 1997

Blank Page

APPROVAL PAGE

LOW FREQUENCY CHARACTERIZATION OF A LOOP ANTENNA

Irene Koukhta

Dr. Edip Niver, Thesis Adviser
Associate Professor of Electrical and Computer Engineering , NJIT

Date

Dr. Gerald Whitman, Committee Member
Professor of Electrical and Computer Engineering, NJIT

Date

Dr. Jacob Savir, Committee Member
Professor of Electrical and Computer Engineering, NJIT

Date

Blank Page

BIOGRAPHICAL SKETCH

Author: Irene Koukhta

Degree: Master of Science

Date: May 1997

Undergraduate and Graduate Education:

- Master of Science in Electrical Engineering,
New Jersey Institute of Technology, Newark, NJ, 1997
- Diploma in Electrical Engineering,
Samara Politechnical Institute, Samara, Russian Federation, 1992

Major: Electrical Engineering

To my beloved family

ACKNOWLEDGMENT

I would like to express sincere gratitude to my supervisor, Dr. Edip Niver, for his guidance, constructive suggestions, friendship, and moral support.

Special thanks are given to Dr. Gerald Whitman and Dr. Jacob Savir for actively participating in my committee.

And finally, the author acknowledges Nikolai Didenko for the timely help and suggestions throughout this research.

TABLE OF CONTENTS

Chapter	Page
1 INTRODUCTION	1
2 LOW FREQUENCY CHARACTERIZATION OF LOOP ANTENNA WITH DELTA-GAP EXCITATION	3
2.1 Integral Equation for the Loop Antenna	3
2.2 Fourier Series Solution of the Integral Equation	6
2.3 Low Frequency Expansion of an Input Admittance	9
3 LOW FREQUENCY CHARACTERIZATION OF A LOOP ANTENNA WITH THE FRILL EXCITATION	13
3.1 Magnetic Frill Excitation of the Loop Antenna	13
3.2 Low Frequency Expansion of Input Admittance for Magnetic Frill Excitation	17
4 NUMERICAL RESULTS	22
4.1 Evaluation of Coefficients	22
4.1 Evaluation of Admittance	25
5 CONCLUSIONS	50
REFERENCES	51

LIST OF TABLES

Table	Page
4.1 Expansion Coefficients for Input Admittance of delta-gap excited loop antenna ...	37
4.1 Expansion Coefficients for Input Admittance of the frill excited loop antenna	49

LIST OF FIGURES

Figure	Page
2.1 Geometry of a Circular Loop Antenna	4
3.1 Half-loop driven through image plane from coaxial transmission line	14
3.2 Equivalent full loop excited by magnetic frill	14
3.3 Detail of geometry	15
4.1 Real and Imaginary components of the normalized current in a delta-gap excited circular loop antenna, $\Omega=10$	26
4.2 Real and Imaginary components of the normalized current in a delta-gap excited circular loop antenna, $\Omega=15$	27
4.3 Normalized Admittance with the Delta-Function Excitation	28
4.4 Comparison of the delta-gap excited antenna input admittance calculated around $k_0=0$, versus Fourier Series Solution	30
4.5 Comparison of the delta-gap excited antenna input admittance calculated around $k_0=0.1$, versus Fourier Series Solution	31
4.6 Comparison of the delta-gap excited antenna input admittance calculated around $k_0=0.2$, versus Fourier Series Solution	32
4.7 Comparison of the delta-gap excited antenna input admittance calculated around $k_0=0.3$, versus Fourier Series Solution	33
4.8 Comparison of the delta-gap excited antenna input admittance calculated around $k_0=0.4$, versus Fourier Series Solution	34
4.9 Comparison of the delta-gap excited antenna input admittance calculated around $k_0=0.5$, versus Fourier Series Solution	35
4.10 Comparison of the delta-gap excited antenna input admittance calculated around $k_0=0.6$, versus Fourier Series Solution	35

LIST OF FIGURES
(continued)

Figure	Page
4.11 Real and Imaginary components of the normalized current in a frill excited circular loop antenna, $\Omega=10$, $a_o=a_i/0.24$	39
4.12 Real and Imaginary components of the normalized current in a frill excited circular loop antenna, $\Omega=15$, $a_o=a_i/0.24$	40
4.13 Normalized Admittance with the Frill Excitation with $\Omega=15$	41
4.14 Comparison of the frill excited antenna input admittance calculated around $k_0=0$, versus Fourier Series Solution	42
4.15 Comparison of the frill excited antenna input admittance calculated around $k_0=0.1$, versus Fourier Series Solution	43
4.16 Comparison of the antenna input admittance calculated around $k_0=0.2$, versus Fourier Series Solution	44
4.17 Comparison of the antenna input admittance calculated around $k_0=0.3$, versus Fourier Series Solution	45
4.18 Comparison of the antenna input admittance calculated around $k_0=0.4$, versus Fourier Series Solution	46
4.19 Comparison of the antenna input admittance calculated around $k_0=0.5$, versus Fourier Series Solution	47
4.20 Comparison of the antenna input admittance calculated around $k_0=0.6$, versus Fourier Series Solution	48

CHAPTER 1

INTRODUCTION

In modern applications the circular loop configuration can either be used as an antenna (receiving or transmitting) in various communication systems or as a probe to detect magnetic fields. A frequency-dependent parametrization of the input admittance of a loop is of interest to the system designer. Especially if the loop has to operate at low frequencies below its first resonance, an accurate representation of an input admittance could not be obtained from elementary delta-gap model of the feed [1]. Conventionally, the input admittance of the loop antenna was determined via the solution based on the delta-gap feed integral equation for the current distribution $I(\varphi)$. Then, the current at the feed point $I(\varphi=0)$ normalized with the voltage V_0^e at the feed point is used to determine the input admittance. The divergent character of the delta-gap model can be corrected by using the feed model in terms of the equivalent magnetic frill current, yielding results which are very close to the experimental measurements [2].

Low frequency expansions of dipole antennas have been obtained by Niver, et. al. [3]. Low frequency expansion of the loop antenna in the form of leading terms have been reported in [1]. Here, a systematic approach to the low frequency characterization of the loop antenna is developed.

The formulation developed in this work leads to the equivalent input admittance of the loop antenna in the form of

$$Y = Y_0 k^0 + Y_1 k + Y_2 k^2 \quad (1.1)$$

and in principle can be extended to include more high order terms if necessary. The advantage of keeping the representation with only few terms permits to associate each term with equivalent inductance, resistance, capacitance and radiation resistance.

CHAPTER 2

LOW FREQUENCY CHARACTERIZATION OF LOOP ANTENNA WITH DELTA-GAP EXCITATION

2.1 Integral Equation for the Loop Antenna

For the convenience in the analysis, the loop antenna shown in Figure 1 will be treated as a transmitting antenna. However, due to reciprocity, all its characteristics will be equally valid if it is used as a receiving antenna. As shown in the Figure 1, it consists of a circular loop of outer radius b of a conducting wire of radius a excited by a voltage generator of time harmonic variation ($e^{j\omega t}$). The generator is assumed to have a voltage V_0^e and is located at the feed point $\varphi'=0$. For low frequency characterization, it will be assumed, that $|ka| \ll 1$ and $a \ll b$, both conditions also satisfy the thin wire approximation [4] commonly used in the literature.

The Electric Field Integral (EFI) equation formulated [4] for the unknown current distribution $I(\varphi)$ along the loop, excited by the voltage generator, based on the vanishing boundary condition defined on the surface of the antenna, i.e., $(\hat{n} \times \bar{E}_{tot})|_S = 0$, except at the feed point. Here $\bar{E}_{tot} = \bar{E}^i + \bar{E}^s$ and \hat{n} is the unit normal vector on the loop surface. At the feed point

$$\int_{-\pi}^{\pi} E_{\varphi}^i b d\varphi = -V_0^e \quad (2.1)$$

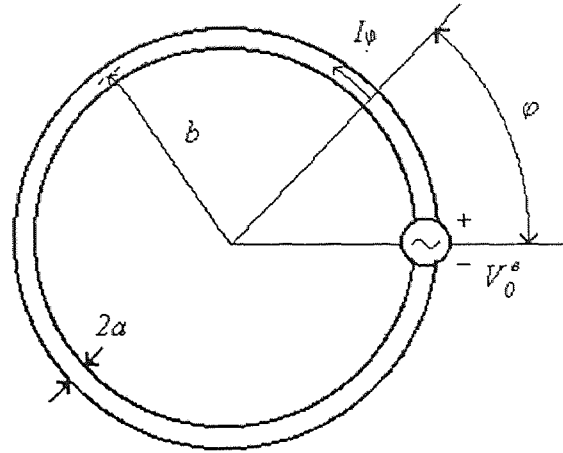


Fig. 2.1 Geometry of a Circular loop antenna

It follows from the relation $-\nabla\Phi = \mathbf{E}^s + j\omega\mathbf{A}$ for the scalar potential that along the surface of the loop

$$\frac{V_0^e \delta(\varphi)}{b} = \frac{1}{r} \frac{\partial \Phi}{\partial \varphi} + j\omega A_\varphi \quad (2.2)$$

The scalar and vector potentials along the antenna surface at the element $ds = b d\varphi$ are given as

$$\Phi = \frac{1}{4\pi\epsilon_0} \int_{-\pi}^{\pi} q(\varphi') W(\varphi - \varphi') d\varphi' \quad (2.3a)$$

$$A_\varphi = \frac{\mu_0}{4\pi} \int_{-\pi}^{\pi} I(\varphi') W(\varphi - \varphi') \cos(\varphi - \varphi') d\varphi' \quad (2.3b)$$

where the kernel is approximated as

$$W(\varphi - \varphi') = \frac{e^{-jkbR}}{R} \quad (2.4a)$$

with

$$R \cong \sqrt{4 \sin^2 \frac{\varphi - \varphi'}{2} + \frac{a^2}{b^2}} \quad (2.4b)$$

Using the continuity equation, $\partial \mathcal{A}(\varphi)/b \partial \varphi + j\omega q(\varphi) = 0$, $q(\varphi)$ in (2.3a) can be eliminated.

This leads to an integral expression for $\frac{\partial \mathcal{A}(\varphi)}{\partial \varphi}$ with the aid of the condition

$$\partial W / \partial \varphi = -\partial W / \partial \varphi'$$

$$\frac{\partial \mathcal{A}(\varphi)}{\partial \varphi} = \frac{j}{4\pi\epsilon_0\omega b} \frac{\partial^2}{\partial \varphi^2} \int_{-\pi}^{\pi} I(\varphi') W(\varphi - \varphi') d\varphi' \quad (2.5)$$

Substitution of (2.3b) and (2.5) in (2.2) results in the approximate integral equation for

the axial current $I(\varphi')$ in the loop subject to (2.4)

$$V_0^e \delta(\varphi) = \frac{j}{4\pi} \int_{-\pi}^{\pi} \left\{ \frac{1}{b\omega\epsilon_0} \frac{\partial^2}{\partial \varphi^2} + \omega b \mu_0 \cos(\varphi - \varphi') \right\} W(\varphi - \varphi') I(\varphi') d\varphi' \quad (2.6)$$

In more compact form (2.6) can be expressed as

$$V_0^e \delta(\varphi) = \frac{j\zeta}{4\pi} \int_{-\pi}^{\pi} M(\varphi - \varphi') I(\varphi') d\varphi' \quad (2.7)$$

where the new kernel $M(\varphi - \varphi')$ is

$$M(\varphi - \varphi') = \left[kb \cos(\varphi - \varphi') + \frac{1}{kb} \frac{\partial^2}{\partial \varphi^2} \right] W(\varphi - \varphi') \quad (2.8)$$

Here, the wave impedance ζ is $\zeta = \omega\mu_0 / k = \sqrt{\mu_0 / \varepsilon_0}$, and the wave number $k = \omega\sqrt{\mu_0\varepsilon_0}$ is defined for the medium (ε_0, μ_0) .

2.2 Fourier Series Solution of the Integral Equation

The solution of the integral equation (2.6) can be obtained in the form of a Fourier series expansion. This solution is based on expansions of both the kernel $W(\varphi - \varphi')$ and the current $I(\varphi)$ in terms of Fourier series

$$W(\varphi - \varphi') = \sum_{-\infty}^{\infty} K_m e^{-jm(\varphi - \varphi')} \quad (2.9)$$

and

$$I(\varphi') = \sum_{-\infty}^{\infty} I_n e^{-jn\varphi'} \quad (2.10)$$

The unknown coefficients K_m and I_n must be determined. Using the inverse relation, I_n can be expressed as

$$I_n = \frac{1}{2\pi} \int_{-\pi}^{\pi} I(\varphi') e^{jn\varphi'} d\varphi' \quad (2.11)$$

Similarly, the unknown expansion coefficients, K_m can be obtained if (2.9) is multiplied on both sides by $e^{jn\varphi}$ and integrated with respect to φ from $-\pi$ to π .

$$\int_{-\pi}^{\pi} W(\varphi - \varphi') e^{jn\varphi} d\varphi = \sum_{-\infty}^{\infty} K_m e^{jm\varphi} \int_{-\pi}^{\pi} e^{j(n-m)\varphi} d\varphi \quad (2.12)$$

Since, in the summation over m only the term $m = n$ contributes to the integral (all other terms vanish), it yields

$$K_n = \frac{1}{2\pi} \int_{-\pi}^{\pi} W(\varphi - \varphi') e^{jn(\varphi - \varphi')} d\varphi = K_{-n} \quad (2.13)$$

The next step is to substitute (2.9) in (2.8) to obtain expansion for the kernel

$$M(\varphi - \varphi') = \frac{kb}{2} [e^{j(\varphi - \varphi')} - e^{-j(\varphi - \varphi')}] \sum_{-\infty}^{\infty} K_m e^{-jm(\varphi - \varphi')} + \frac{1}{kb} \frac{\partial^2}{\partial \Phi^2} \sum_{-\infty}^{\infty} K_m e^{-jm(\varphi - \varphi')} \quad (2.14)$$

Since

$$\sum_{-\infty}^{\infty} K_m e^{-j(m-1)(\varphi - \varphi')} = \sum_{-\infty}^{\infty} K_{n+1} e^{-jn(\varphi - \varphi')} \quad (2.15)$$

and

$$\sum_{-\infty}^{\infty} K_m e^{-j(m+1)(\varphi - \varphi')} = \sum_{-\infty}^{\infty} K_{n-1} e^{-jn(\varphi - \varphi')} \quad (2.16)$$

it is evident that

$$M(\varphi - \varphi') = \sum_{-\infty}^{\infty} a_n e^{-jn(\varphi - \varphi')} \quad (2.17)$$

where

$$a_n = \frac{kb}{2} (K_{n+1} + K_{n-1}) - \frac{n^2}{kb} K_n = a_{-n} \quad (2.18)$$

Hence, the integral equation in (2.7) reduces to

$$V_0^e \mathcal{A}(\varphi) = \frac{j\zeta}{4\pi} \sum_{-\infty}^{\infty} a_n \int_{-\pi}^{\pi} e^{-n(\varphi - \varphi')} I(\varphi') d\varphi' \quad (2.19)$$

Substitution of the expansion for current $I(\phi')$ in (2.10) and (2.7) into (2.19) leads to

$$V_0^e \delta(\varphi) = \frac{j\zeta}{2} \sum_{-\infty}^{\infty} a_n I_n e^{-jn\varphi} \quad (2.20)$$

Expansion in (2.20) represents a Fourier series with the expansion coefficients $(j\zeta/2)a_n I_n$.

The coefficients are determined using the properties of the δ -function

$$\frac{j\zeta a_n I_n}{2} = \frac{1}{2\pi} \int_{-\pi}^{\pi} V_0^e \delta(\varphi) e^{jn\varphi} d\varphi = \frac{V_0^e}{2\pi} \quad (2.21)$$

and explicitly can be expressed as

$$I_n = -\frac{jV_0^e}{\zeta\pi a_n} \quad (2.22)$$

The infinite summation in (2.10) can be re-expressed using only non-negative indices n to give for unknown current distributions

$$I(\varphi') = \sum_{-\infty}^{\infty} I_n e^{-jn\varphi'} = \sum_{-\infty}^{\infty} \left(-\frac{jV_0^e}{\zeta\pi a_n} e^{-jn\varphi'} \right) = -\frac{jV_0^e}{\zeta\pi} \left\{ \frac{1}{a_0} + \sum_1^{\infty} \frac{1}{a_n} (e^{-jn\varphi'} + e^{jn\varphi'}) \right\} \quad (2.23)$$

and can be reduced further into the solution for the unknown current distribution on

$$I(\varphi') = -\frac{jV_0^e}{\zeta\pi} \left(\frac{1}{a_0} + 2 \sum_1^{\infty} \frac{1}{a_n} \cos n\varphi' \right) \quad (2.24)$$

The current distribution evaluated at the feed point, $\varphi'=0$ leads to the input admittance of the loop

$$Y = \frac{I(0)}{V_0^e} = -\frac{j}{\zeta\pi} \left(\frac{1}{a_0} + 2 \sum_1^{\infty} \frac{1}{a_n} \right) \quad (2.25)$$

2.3 Low Frequency Expansion of an Input Admittance

A frequency dependent analytical expression for the input admittance of a loop antenna is desirable for circuit design applications. Here, the input admittance expansion in terms of wavenumber k is formulated, i.e. $Y=Y(k)$. Since the input admittance Y in (2.25) depends on the values of α_0 and a_n inversely, and (2.18) yields

$$\frac{1}{\alpha_0} = \frac{1}{kb} \frac{1}{K_1(k)} \quad (2.26)$$

the presence of a singularity at $k = 0$ necessitates the proper consideration of the expansion around $k_0 = 0$.

Using the Taylor's series expansion of an analytical function $f(x)$ around an expansion point x_0 ,

$$f(x) = f(x_0) + \frac{1}{1!} \left. \frac{\partial f(x)}{\partial x} \right|_{x=x_0} (x-x_0) + \frac{1}{2!} \left. \frac{\partial^2 f(x)}{\partial x^2} \right|_{x=x_0} (x-x_0)^2 + \frac{1}{3!} \left. \frac{\partial^3 f(x)}{\partial x^3} \right|_{x=x_0} (x-x_0)^3 + \quad (2.27)$$

suggests that the lower order coefficient $1/\alpha_0$ given in (2.26) can be expanded around an expansion frequency $k = k_0$. Thus,

$$\begin{aligned} \frac{1}{\alpha_0} &= C_0 + C_1(k - k_0) + C_2(k - k_0)^2 = \\ &= (C_0 - C_1 k_0 + C_2 k_0^2) + (C_1 - 2C_2 k_0)k + C_2 k^2 \end{aligned} \quad (2.28)$$

where expansion coefficients are expressed as

$$C_0 = b^{-1} k_0^{-1} K_1^{-1}(k_0) \quad (2.29a)$$

$$C_1 = b^{-1} \{ -k_0^{-2} K_1^{-1}(k_0) - k_0^{-1} K_1^{-2}(k_0) K_1'(k_0) \} \quad (2.29b)$$

$$C_2 = (2b)^{-1} \{ 2k_0^{-3} K_1^{-1}(k_0) + k_0^{-2} K_1^{-2}(k_0) K_1'(k_0) + \\ + k_0^{-2} K_1^{-2}(k_0) K_1'(k_0) + 2k_0^{-1} K_1^{-3}(k_0) (K_1'(k_0))^2 - k_0^{-1} K_1^{-2}(k_0) K_1''(k_0) \} \quad (2.29c)$$

The derivatives of the expansion coefficients K_1 are defined as

$$K_1'(k_0) = -\frac{jb}{2\pi} \int_{-\pi}^{\pi} e^{j\theta} e^{-jk_0 b R(\theta)} d\theta \quad (2.30)$$

and

$$K_1''(k_0) = -\frac{b^2}{2\pi} \int_{-\pi}^{\pi} R(\theta) e^{j\theta} e^{-jk_0 b R(\theta)} d\theta \quad (2.31)$$

Since, the function $\frac{1}{a_0(k)} = \frac{1}{kb} \frac{1}{K_1(k)}$ has a singular point at $k = 0$, which requires

that a term $\sim 1/k$ appears in the series expansion of $1/a_0$. The Taylor's series then reduces to a MacLaurin's series when the expansion point is chosen at $k_0 = 0$, hence

$$\frac{1}{a_0} = A_{-1} k^{-1} + A_0 + A_1 k + A_2 k^2 \quad (2.32)$$

where the expansion coefficients are

$$A_{-1} = b^{-1} K_1^{-1}(0) \quad (2.33a)$$

$$A_0 = b^{-1} K_1^{-2}(0) K_1'(0) \quad (2.33b)$$

$$A_1 = (2b)^{-1} \{ -K_1^{-2}(0) K_1''(0) \} \quad (2.33c)$$

$$A_2 = (6b)^{-1} \{ 4K_1^{-3}(0) K_1''(0) + K_1^{-2}(0) K_1'''(0) \} \quad (2.33d)$$

Usage of (2.27) for expansion point $k_0 = 0$ requires the additional third derivative K_1''' , and

$$K_1'(0) = -\frac{jb}{2\pi} \int_{-\pi}^{\pi} e^{j\theta} d\theta = \frac{b}{2\pi} (e^{j\pi} - e^{-j\pi}) = 0 \quad (2.34)$$

and

$$K_1''(0) = -\frac{b^2}{2\pi} \int_{-\pi}^{\pi} R(\theta) e^{j\theta} d\theta \quad (2.35)$$

and

$$K_1'''(0) = \frac{jb^3}{2\pi} \int_{-\pi}^{\pi} R^2(\theta) e^{-j\theta} d\theta \quad (2.36)$$

High order expansion coefficients $1/a_n(k)$ can also be expanded using a similar procedure. Following (2.18), $1/a_n$ in (2.25) is expressed as

$$1/a_n = 1/\left\{\frac{kb}{2}(K_{n+1} + K_{n-1}) - \frac{n^2}{kb}K_n\right\} \quad (2.37)$$

As $1/a_n$ has no singularities for any k , the Taylor's series expansion can be written directly as

$$\begin{aligned} \frac{1}{a_n} &= B_{0n} + B_{1n}(k - k_0) + B_{2n}(k - k_0)^2 = \\ &= (B_{0n} - B_{1n}k_0 + B_{2n}k_0^2) + (B_{1n} - 2B_{2n}k_0)k + B_{2n}k^2 \end{aligned} \quad (2.38)$$

where

$$B_{0n} = 1/a_n(k_0) \quad (2.39a)$$

$$B_{1n} = -a_n^{-2}(k_0) a_n'(k_0) \quad (2.39b)$$

$$B_{2n} = 1/2 \{2 a_n^{-3}(k_0)(a_n'(k_0))^2 - a_n^{-2}(k_0)a_n''(k_0)\} \quad (2.39c)$$

with explicit expressions for the individual terms

$$a_n(k_0) = \frac{k_0 b}{2} \{K_{n+1}(k_0) + K_{n-1}(k_0)\} - \frac{n^2}{k_0 b} K_n(k_0) \quad (2.40)$$

$$\begin{aligned}
a_n'(k_0) &= \frac{b}{2} \{K_{n+1}(k_0) + K_{n-1}(k_0)\} + \frac{k_0 b}{2} \{K_{n+1}'(k_0) + K_{n-1}'(k_0)\} - \\
&\quad - \left\{ \frac{n^2}{k_0 b} K_n(k_0) + \frac{n^2}{k_0 b} K_n'(k_0) \right\} \quad (2.41)
\end{aligned}$$

$$\begin{aligned}
a_n''(k_0) &= \frac{b}{2} \{K_{n+1}'(k_0) + K_{n-1}'(k_0)\} 2 + \frac{k_0 b}{2} \{K_{n+1}''(k_0) + K_{n-1}''(k_0)\} - \\
&\quad - \left\{ \frac{2n^2}{k_0^3 b} K_n(k_0) - \frac{n^2}{k_0 b} K_n'(k_0) 2 + \frac{n^2}{k_0 b} K_n''(k_0) \right\} \quad (2.42)
\end{aligned}$$

Special consideration has to be taken when chosen expansion point is $k_0 = 0$, the Taylor series then reduces to the MacLaurin's series

$$\frac{1}{a_n} = E_{0n} + E_{1n}k + E_{2n}k^2 \quad (2.43)$$

with expansion coefficients defined as

$$E_{0n} = a_n^{-1}(0) = 0 \quad (2.44a)$$

$$E_{1n} = -b / (n^2 K_n(0)) \quad (2.44b)$$

$$E_{2n} = -2b K_n'(0) / (n^2 K_n'(0))^2 \quad (2.44c)$$

Using all these expansions, the input admittance, expressed in ascending order of terms in k around the expansion point $k_0 = 0$, becomes

$$Y = \frac{1}{j\zeta\pi} A_{-1} \frac{1}{k} + \frac{1}{j\zeta\pi} \sum_{n=1}^{\infty} E_{0n} + \frac{1}{j\zeta\pi} (-A_1 + \sum_{n=1}^{\infty} E_{1n})k + \frac{1}{j\zeta\pi} (A_2 + \sum_{n=1}^{\infty} E_{2n})k^2 \quad (2.45)$$

and if the chosen expansion point is $k_0 \neq 0$, is given by

$$\begin{aligned}
Y &= \frac{1}{j\zeta\pi} (C_0 - C_1 k_0 + C_2 k_0^2) + \frac{1}{j\zeta\pi} \sum_{n=1}^{\infty} (B_{0n} - B_{1n} k_0 + B_{2n} k_0^2) + \\
&\quad + \frac{1}{j\zeta\pi} (C_1 - 2k_0 C_2 + 2 \sum_{n=1}^{\infty} (B_{1n} - 2k_0 B_{2n}))k + \frac{1}{j\zeta\pi} (C_2 + 2 \sum_{n=1}^{\infty} B_{2n})k^2 \quad (2.46)
\end{aligned}$$

CHAPTER 3

LOW FREQUENCY CHARACTERIZATION OF A LOOP ANTENNA WITH THE FRILL EXCITATION

The use of the δ -gap generator in feed modeling leads to a well known problem, the imaginary part of the series for the current diverges at the feed point: $\text{Im}\{I(0)\} = \text{Im}\left\{\sum_n I_n(\phi')\right\} \rightarrow \infty$ as $n \rightarrow \infty$ due to the divergent nature of the chosen expansion. However, a simple delta-gap model of the feed point in terms of the parallel plate capacitance $C = \epsilon_0 \frac{A}{d}$ suggests that $d \rightarrow 0, C \rightarrow \infty$. The divergent nature of the susceptance due to the δ -gap feed model can be improved by using a more realistic model for the excitation of the loop antenna in terms of an equivalent frill magnetic current generator [2].

3.1 Magnetic Frill Excitation of the Loop Antenna

A loop antenna in free space can be replaced by a half-loop fed through a perfectly conducting plane, as shown in Fig. 3.1. The electric field in the coaxial aperture is assumed to be a TEM mode:

$$E_\rho(\rho) = V_0 / [\rho \ln(a_0/a_i)], \quad a_i \leq \rho \leq a_0 \quad (3.1)$$

where ρ is the radial coordinate on the conducting plane, a_i and a_0 are the inner and outer radii of the coaxial transmission line, respectively. The radius of the outer conductor a_0 is chosen small enough that only the TEM mode propagates in the coaxial line. The

electromagnetic analysis of the structure in Fig. 3.2 facilitates solution of the antenna depicted in the Fig. 3.1 due to the presence of a large conducting plane, assumed to be infinite and the use of image theory.

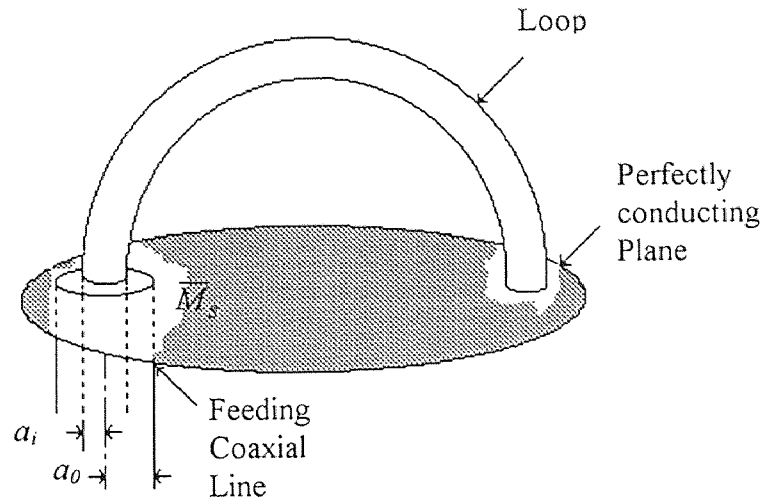


Fig. 3.1 Half-loop driven through image plane from coaxial transmission line.

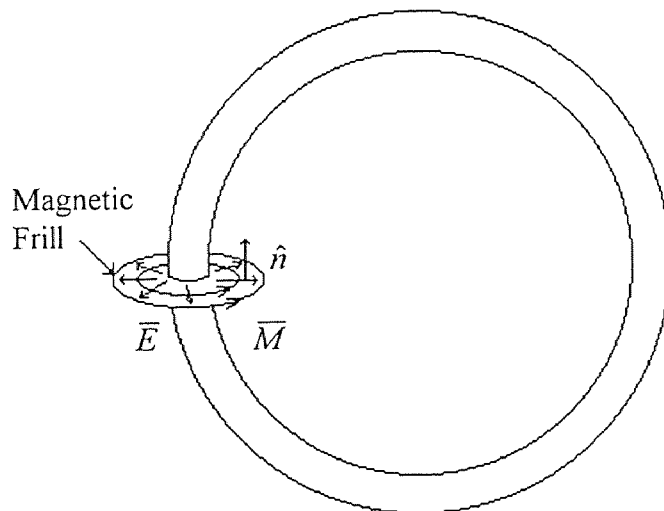


Fig. 3.2 Equivalent full loop excited by magnetic frill

Here, the loop antenna is driven by a magnetic frill with magnetic surface current density

$$\vec{M}_s = \hat{n} \times \vec{E}^i = -2V_0 \Lambda [\rho' \ln(a_0/a_i)] \hat{\theta}', \quad a_i \leq \rho' \leq a_0 \quad (3.2)$$

The electric field produced by this magnetic frill current along the surface of the loop serves as the excitation for the antenna [5].

$$E^i = -\frac{1}{4\pi} \iiint_s M_s \times \nabla'^i \psi \, dS' \quad (3.3)$$

where the free space Green's function is

$$\psi = \frac{e^{-jkr}}{r} \quad (3.4)$$

and, referring to Fig. 3.3, r is the distance from the source point A (toroidal coordinates: $\rho', \theta', \phi' = 0$) on the frill to the observation point B ($\rho = a_i, \theta, \phi$) on the surface of the loop. The prime “'” in ∇' indicates differentiation with respect to the source variables, and the surface of integration is the area filled by the equivalent frill current density.

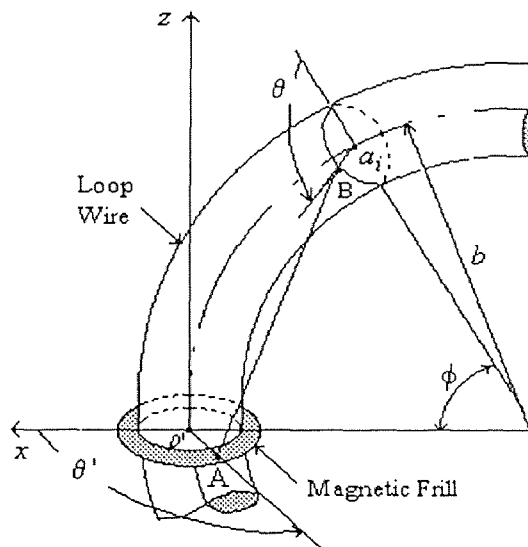


Fig. 3.3 Detail of geometry

The field produced by the frill current is most significant in the vicinity of the driving point, $\varphi = 0$. Due to the thin-wire assumption, the wire of the loop is nearly straight in this region, and the distance r can be approximated by

$$r \approx \sqrt{4b^2 \sin^2(\varphi/2) + a_i^2 + \rho'^2 - 2a_i \rho' \cos \chi} \quad (3.5)$$

with $\chi = \theta - \theta'$. In addition, the component of the electric field tangential to the surface of the loop E_φ^i is approximately equal to

$$E_\varphi^i \approx E_z \cos \varphi \quad (3.6)$$

After inserting (3.2) into (3.3) and expressing ∇' in terms of the source coordinates (ρ', θ', z') , E_φ^i reduces to

$$\begin{aligned} E_\varphi^i(\varphi) &= \frac{-V_0 \cos \varphi}{2\pi \ln(a_0/a_i)} \int_{-\pi}^{\pi} \int_{a_i}^{a_0} \frac{\partial \psi}{\partial \rho} d\rho' d\chi = \\ &= \frac{-V_0 \cos \varphi}{2\pi \ln(a_0/a_i)} \int_{-\pi}^{\pi} [\psi(\rho' = a_0) - \psi(\rho' = a_i)] d\chi \end{aligned} \quad (3.7)$$

Hence, the electric field integral equation in (2.7) with the inclusion of magnetic frill current becomes

$$V_0^e \delta(\varphi) = \frac{j\zeta}{4\pi} \int_{-\pi}^{\pi} M(\varphi - \varphi') I(\varphi') d\varphi' \quad (3.8)$$

Similarly, expanding the current $I(\varphi')$ along the loop in terms of the Fourier series (2.10) leads to

$$E_\varphi^i(\varphi) = \frac{j\zeta}{2} \sum_{n=-\infty}^{\infty} a_n I_n e^{-jn\varphi} \quad (3.9)$$

where the coefficients are given by

$$\frac{j\zeta a_n I_n}{2} = \frac{1}{2\pi} \int_{-\pi}^{\pi} E_{\varphi}^i e^{jn\varphi} d\varphi = b_n \quad (3.10)$$

Extracting current expansion coefficients I_n as

$$I_n = \frac{2}{j\zeta} \left(\frac{b_n}{a_n} \right) \quad (3.11)$$

the unknown current $I(\varphi')$ can then be explicitly expressed as

$$I(\varphi') = \sum_{-\infty}^{\infty} I_n e^{-jn\varphi'} = \sum_{-\infty}^{\infty} \frac{2}{j\zeta} \frac{b_n}{a_n} e^{-jn\varphi'} = \frac{2}{j\zeta} \left\{ \frac{b_0}{a_0} + \sum_1^{\infty} \frac{b_n}{a_n} (e^{-jn\varphi'} + e^{jn\varphi'}) \right\} \quad (3.12)$$

and the final result for the desired series of current reduces

$$I(\varphi) = \frac{2}{j\zeta} \left(\frac{b_0}{a_0} + 2 \sum_1^{\infty} \frac{b_n}{a_n} \cos n\varphi' \right) \quad (3.13)$$

The corresponding input admittance is

$$Y = \frac{I(0)}{V_0} = \frac{2}{j\zeta V_0} \left(\frac{b_0}{a_0} + 2 \sum_1^{\infty} \frac{b_n}{a_n} \right) \quad (3.14)$$

3.2 Low Frequency Expansion of an Input Admittance for Magnetic Frill Excitation

The frequency characterization of an input admittance of a loop antenna modeled by a magnetic frill excitation consists of a series representation of an admittance as a function of $k = \omega/c$, where c is the speed of light in vacuum. If only few terms kept in a such expansion of an admittance

$$Y(\omega) = 1/j\omega L + G + j\omega C + \omega^2 P + j\omega^3 Q \quad (3.15)$$

the expansion coefficients will correspond to capacitance, resistance, inductance, radiation resistance and radiation reactance. However, confining such an expansion to only a few terms, limits the applicability of this characterization over relatively narrow frequency band. The lowest expansion point can be chosen as $k_0 = 0$. If a wider band coverage is desired then the expansion has to be implemented over the band repeatedly at different expansion points $k = k_0$. The expansion of (3.14) can be accomplished by expanding b_0/a_0 and b_n/a_n separately.

Using the Taylor's series expansion around k_0 in (2.27), the ratio $b_0(k)/a_0(k)$ can be expressed as

$$\frac{b_0(k)}{a_0(k)} = \left. \left(\frac{b_0(k)}{a_0(k)} \right) \right|_{k=k_0} + \left. \frac{\partial}{\partial k} \left(\frac{b_0(k)}{a_0(k)} \right) \right|_{k=k_0} (k - k_0) + \frac{1}{2} \left. \frac{\partial^2}{\partial k^2} \left(\frac{b_0(k)}{a_0(k)} \right) \right|_{k=k_0} (k - k_0)^2 \quad (3.16)$$

or it can be rearranged as

$$\begin{aligned} \frac{b_0(k)}{a_0(k)} &= D_0 + D_1(k - k_0) + D_2(k - k_0)^2 = \\ &= (D_0 - D_1 k_0 + D_2 k_0^2) + (D_1 - 2D_2 k_0)k + D_2 k^2 \end{aligned} \quad (3.17)$$

where,

$$D_0 = b_0(k_0) a_0^{-1}(k_0) \quad (3.18a)$$

$$D_1 = a_0^{-2}(k_0) \{ b_0'(k_0) a_0(k_0) + b_0(k_0) a_0'(k_0) \} \quad (3.18b)$$

$$\begin{aligned} D_2 = 1/2 \{ -2a_0^{-3}(k_0) a_0'(k_0) (b_0'(k_0) a_0(k_0) + b_0(k_0) a_0'(k_0)) + \\ + a_0^{-2}(k_0) (b_0''(k_0) a_0(k_0) - b_0(k_0) a_0''(k_0)) \} \end{aligned} \quad (3.18c)$$

From (4.2)

$$b'_n(k_0) = \frac{jV_0}{4\pi^2 \ln\left(\frac{a_0}{a_i}\right)} \int_{-\pi}^{\pi} \int_{-\pi}^{\pi} (e^{-jk_0 r_1} - e^{-jk_0 r_2}) \cos\varphi \cos n\varphi d\chi d\varphi \quad (3.19)$$

$$b''_n(k_0) = \frac{V_0}{4\pi^2 \ln\left(\frac{a_0}{a_i}\right)} \int_{-\pi}^{\pi} \int_{-\pi}^{\pi} (r_1 e^{-jk_0 r_1} - r_2 e^{-jk_0 r_2}) \cos\varphi \cos n\varphi d\chi d\varphi \quad (3.20)$$

where distance r_1 and r_2 are defined respectively, as

$$r_1 = \sqrt{4b^2 \sin^2 \varphi / 2 + a_i^2 + a_0^2 - 2a_i a_0 \cos \chi} \quad (3.21)$$

and

$$r_2 = \sqrt{4b^2 \sin^2 \varphi / 2 + 4a_i^2 \sin^2 \chi / 2} \quad (3.22)$$

The function $\frac{b_0(k)}{a_0(k)} = \frac{1}{kb} \frac{b_0(k)}{K_1(k)}$ has a singular point at $k = 0$, therefore a term $\sim 1/k$

has to be included in the series expansion of $b_0(k)/a_0(k)$. The coefficients of the series can be easily evaluated by expanding $b_0(k)/(bK_1(k))$ in a Taylor series and dividing the result by k . Hence, such an expansion can be expressed as

$$\frac{b_0(k)}{a_0(k)} = N_{-1} \frac{1}{k} + N_0 + N_1 k + N_2 k^2 \quad (3.23)$$

where

$$N_{-1} = b^{-1} b_0(0) K_1^{-1}(0) \quad (3.24a)$$

$$N_0 = b^{-1} K_1^{-2}(0) \{ b_0'(0) K_1(0) - b_0(0) K_1'(0) \} \quad (3.24b)$$

$$N_1 = (2b)^{-1} \{ -2 K_1'(0) K_1^{-3}(0) (b_0'(0) K_1(0) - b_0(0) K_1'(0)) + K_1^{-2}(0) (b_0''(0) K_1(0) - b_0(0) K_1''(0)) \} \quad (3.24c)$$

$$\begin{aligned}
N_2 = & (6b)^{-1} \{ 6(K_1'(0))^2 K_1^{-4}(0) (b_0'(0)K_1(0) - b_0(0)K_1'(0)) - \\
& - 4K_1'(0) K_1^{-3}(0) (b_0''(0)K_1(0) - b_0(0)K_1''(0)) + \\
& + K_1^{-2}(0) (b_0'''(0)K_1(0) - b_0''(0)K_1'(0) - b_0'(0)K_1''(0) - b_0(0)K_1'''(0)) \} \quad (3.24d)
\end{aligned}$$

Similarly the ratio $b_n(k)/a_n(k)$ can be expanded in terms of a Taylor series around k_0 as

$$\begin{aligned}
b_n(k)/a_n(k) &= F_{0n} + F_{1n}(k-k_0) + F_{2n}(k-k_0)^2 = \\
&= (F_{0n} - F_{1n}k_0 + F_{2n}k_0^2) + (F_{1n} - 2F_{2n}k_0)k + F_{2n}k^2 \quad (3.25)
\end{aligned}$$

where,

$$F_{0n} = b_n(k_0)a_n^{-1}(k_0) \quad (3.26a)$$

$$F_{1n} = a_n^{-2}(k_0) \{ b_n'(k_0)a_n(k_0) + b_n(k_0)a_n'(k_0) \} \quad (3.26b)$$

$$\begin{aligned}
F_{2n} = & 1/2 \{ -2a_n^{-3}(k_0)a_n'(k_0)(b_n'(k_0)a_n(k_0) + b_n(k_0)a_n'(k_0)) + \\
& + a_n^{-2}(k_0)(b_n''(k_0)a_n(k_0) - b_n(k_0)a_n''(k_0)) \} \quad (3.26c)
\end{aligned}$$

Similarly, if the expansion is carried around $k_0 = 0$ equation in (3.25) simplifies as

$$\frac{b_n(k)}{a_n(k)} = \left(\frac{b_n(k)}{a_n(k)} \right) \Big|_{k=0} + \frac{\partial}{\partial k} \left(\frac{b_n(k)}{a_n(k)} \right) \Big|_{k=0} k + \frac{1}{2} \frac{\partial^2}{\partial k^2} \left(\frac{b_n(k)}{a_n(k)} \right) \Big|_{k=0} k^2 \quad (3.27)$$

and can be equated to

$$\frac{b_n(k)}{a_n(k)} = M_{0n} + M_{1n}k + M_{2n}k^2 \quad (3.28)$$

Using (2.18) it can be expressed as

$$\frac{b_n(k)}{a_n(k)} = \frac{b_n}{k b \frac{2}{(K_{n+1} + K_{n-1}) - \frac{n^2}{k b} K_n}} = \frac{k b b_n}{k^2 b^2 \frac{2}{(K_{n+1} + K_{n-1}) - n^2 K}} = \frac{k b b_n}{d_n(k)} \quad (3.29)$$

where individual terms are

$$d_n(k) = k^2 b^2 (K_{n+1}(k) + K_{n-1}(k))/2 - n^2 K_n(k) \quad (3.30)$$

$$d_n' = kb^2(K_{n+1}(k) + K_{n-1}(k)) + k^2b^2(K_{n+1}'(k) + K_{n-1}'(k))/2 - n^2K_n'(k) \quad (3.31)$$

$$(b_n(k)/\alpha_n(k))' = (bb_n(k) + kbb_n'(k))d_n - kbb_n d_n'(k) / d_n^2(k) \quad (3.32)$$

$$\begin{aligned} (b_n/\alpha_n)'' = & (2bb_n'(k) + kbb_n''(k))d_n(k) - (bb_n(k) + kbb_n'(k))d_n'(k) / d_n^2(k) + \\ & + (bb_n d_n'(k) + kbb_n' d_n'(k) + kbb_n d_n''(k))d_n^2(k) - \\ & - 2d_n(k)d_n'(k)kbb_n d_n'(k) / d_n^4(k) \end{aligned} \quad (3.33)$$

Comparison of (3.26) and (3.27) leads to

$$M_{0n} = b_n(0)\alpha_n^{-1}(0) = 0 \quad (3.34a)$$

$$M_{1n} = -bb_n(0) / (n^2K_n(0)) \quad (3.34b)$$

$$M_{2n} = -2b(b_n'(0)K_n(0) - b_n(0)K_n'(0)) / (n^2K_n'(0))^2 \quad (3.34c)$$

Then, the input admittance for the case when $k_0 \neq 0$, becomes

$$\begin{aligned} Y = & \frac{2}{j\zeta V_0}(D_0 - D_1 k_0 + D_2 k_0^2) + \frac{2}{j\zeta V_0} \sum_{n=1}^{\infty} (F_{0n} - F_{1n} k_0 + F_{2n} k_0^2) + \\ & + \frac{2}{j\zeta V_0} (D_1 - 2k_0 D_2 + 2 \sum_{n=1}^{\infty} (F_{1n} - 2k_0 F_{2n}))k + \frac{2}{j\zeta V_0} (D_2 + 2 \sum_{n=1}^{\infty} F_{2n})k^2 \end{aligned} \quad (3.35)$$

and for $k_0 = 0$ the input admittance reduces to

$$Y = \frac{2}{j\zeta V_0} N_{-1} \frac{1}{k} + \frac{2}{j\zeta V_0} (N_0 + 2 \sum_{n=1}^{\infty} M_{0n}) + \frac{2}{j\zeta V_0} (N_1 + 2 \sum_{n=1}^{\infty} M_{1n})k + \frac{2}{j\zeta V_0} (N_2 + 2 \sum_{n=1}^{\infty} M_{2n})k^2 \quad (3.36)$$

CHAPTER 4

NUMERICAL RESULTS

4.1 Evaluation of Coefficients

The expansion coefficients I_n in $I(\varphi')$ need the evaluation of a_n (see 2.22) which are expressed in terms of K_n given in (2.13),

$$K_n = \frac{1}{2\pi} \int_{-\pi}^{\pi} e^{jn\theta} e^{jk_0 b R(\theta)} \frac{d\theta}{R(\theta)} \quad (4.1)$$

where $\theta = (\varphi - \varphi')$, $R(\theta) = [4\sin^2(\theta/2) + a^2/b^2]^{1/2}$.

Integration in evaluating the expansion coefficients is carried out using Simpson method. However for a loop antenna these coefficients could have been evaluated analytically and expressed in terms of Bessel functions. Numerical integration was preferred to keep the programming simpler by avoiding inclusion of special subroutines to evaluate Bessel's functions.

Similarly, to obtain the current distribution $I(\varphi)$ in the loop with the magnetic frill excitation, the coefficients b_n defined in (3.10) have to be evaluated

$$b_n = -\frac{V_0}{4\pi^2 \ln(a_0/a_n)} \int_{-\pi}^{\pi} \int_{-\pi}^{\pi} \left\{ \frac{\exp[-jk\sqrt{4b^2 \sin^2(\varphi/2) + a_i^2 + a_0^2 - 2a_i a_0 \cos(\chi)}]}{\sqrt{4b^2 \sin^2(\varphi/2) + a_i^2 + a_0^2 - 2a_i a_0 \cos(\chi)}} \right. \\ \left. - \frac{\exp[-jk\sqrt{4b^2 \sin^2(\varphi/2) + 4a_i^2 \sin^2(\chi/2)}]}{\sqrt{4b^2 \sin^2(\varphi/2) + 4a_i^2 \sin^2(\chi/2)}} \right\} \cos\varphi \cos(n\varphi) d\chi d\varphi \quad (4.2)$$

In order to determine numerical values of these coefficients a combination of analytical evaluation and numerical integration is used. The purpose of analytical evaluation is to reduce computational burden of a two dimensional integration by simplifying the integrand and by integrating with respect of χ analytically. The remaining integral with respect of φ is evaluated numerically.

Hence, the expression for b_n can be modified

$$b_n = \frac{-V_0}{4\pi^2 \ln(a_0/a_i)} \int_{-\pi}^{\pi} \int_{-\pi}^{\pi} [\Psi(\rho' = a_0) - \Psi(\rho' = a_i)] d\chi \cos\varphi \cos(n\varphi) d\varphi \quad (4.3)$$

Then the function $\Psi(\rho')$ can be expanded in a Taylor series with respect of ρ' as

$$\Psi(\rho' = a_0) = \Psi(0) + \Psi'(0) a_0 + 1/2\Psi''(0) a_0^2 \quad (4.4)$$

and

$$\Psi(\rho' = a_i) = \Psi(0) + \Psi'(0) a_i + 1/2\Psi''(0) a_i^2 \quad (4.5)$$

Since,

$$\frac{\partial \Psi}{\partial \rho} = \frac{\partial \Psi}{\partial r} \cdot \frac{\partial r}{\partial \rho} \quad (4.6)$$

then,

$$\frac{\partial^2 \Psi}{\partial \rho^2} = \frac{\partial}{\partial \rho} \left\{ \frac{\partial \Psi}{\partial r} \frac{\partial r}{\partial \rho} \right\} = \frac{\partial r}{\partial \rho} \cdot \frac{\partial}{\partial r} \left[\frac{\partial \Psi}{\partial r} \right] \cdot \frac{\partial r}{\partial \rho} + \frac{\partial \Psi}{\partial r} \frac{\partial^2 r}{\partial \rho^2} = \frac{\partial^2 \Psi}{\partial r^2} \left(\frac{\partial r}{\partial \rho} \right)^2 + \frac{\partial \Psi}{\partial r} \frac{\partial^2 r}{\partial \rho^2} \quad (4.7)$$

where

$$\frac{\partial r}{\partial \rho} = \frac{\rho - a_i \cos \chi}{\sqrt{4b^2 \sin^2(\varphi/2) + a_i^2 + \rho^2 - 2a_i \rho \cos \chi}} = \frac{\rho - a_i \cos \chi}{r} \quad (4.8)$$

$$\frac{\partial \Psi}{\partial r} = -j\beta \frac{e^{-j\beta r}}{r} - \frac{e^{-j\beta r}}{r^2} = (-j\beta - 1/r)\Psi \quad (4.9)$$

$$\begin{aligned} \frac{\partial^2 r}{\partial \rho^2} &= \frac{r \frac{\partial}{\partial \rho} (\rho - a_i \cos \chi) - (\rho - a_i \cos \chi) \frac{\partial r}{\partial \rho}}{r^2} = \\ &= \frac{r - (\rho - a_i \cos \chi)^2 / r}{r^2} = \frac{1}{r} - \frac{(\rho - a_i \cos \chi)}{r^3} \end{aligned} \quad (4.10)$$

$$\begin{aligned} \frac{\partial^2 \Psi}{\partial r^2} &= (-j\beta - 1/r) \frac{\partial \Psi}{\partial r} + \Psi \frac{\partial}{\partial r} (j\beta - 1/r) = \\ &= (-j\beta - 1/r)^2 \Psi + \Psi 1/r^2 = ((-j\beta - 1/r)^2 + 1/r^2) \Psi \end{aligned} \quad (4.11)$$

$$\begin{aligned} \frac{\partial^2 \Psi}{\partial \rho^2} &= ((-j\beta - 1/r)^2 - 1/r^2) \frac{(\rho - a_i \cos \chi)^2}{r^2} \Psi + \\ &+ (-j\beta - 1/r)(1/r - (\rho - a_i \cos \chi)^2 / r^3) \Psi \end{aligned} \quad (4.12)$$

The first derivative of Ψ with respect of ρ at $\rho=0$ and integrated with respect to χ from $-\pi$ to π is equal to zero. The second derivative of Ψ with respect of ρ at $\rho=0$ and integrated with respect of χ from $-\pi$ to π is equal to

$$\begin{aligned} \int_{-\pi}^{\pi} \frac{\partial^2 \Psi}{\partial \rho^2} \Big|_{\rho=0} d\chi &= \frac{e^{-j\beta r(0)}}{r(0)} ((-j\beta - 1/r(0))^2 - 1/r^2(0)) \frac{a_i^2 \pi}{r^2(0)} + \\ &+ \frac{e^{-j\beta r(0)}}{r(0)} (-j\beta - 1/r(0))(2\pi / r(0) - \pi / r^3(0)) \end{aligned} \quad (4.13)$$

where $r(0) = r(\rho=0)$.

Therefore, use of (4.13) in evaluation of the coefficients b_n reduces the computational effort significantly.

4.2 Evaluation of Admittance

Computer codes were developed to analyze the input admittance of loop antenna with source modeled via

- (a) delta-gap generator,
- (b) magnetic frill current excitation .

Frequency characterization of admittance expressed through various expansions in this work are compared to Fourier series solutions reported in [1] and [2] for the delta-gap and magnetic frill excitations, respectively. These solutions were used as a reference to compare results based on various characterizations developed throughout the scope of this work. Computer codes were written to duplicate results reported in [1] and [2]. Figure 4.1 and 4.2 show the variation of the current distribution for the delta-gap excitation as a function of φ along the loop antenna for $\Omega = 2 \ln (2\pi b/a)$, $\Omega = 10$ and $\Omega = 15$, respectively. Figure 4.1 exhibits identical variation as in with the Figure 11.4 reported in [4].

Using the derived current distributions in the computer codes , the input admittance Y is determined and shown in Figure 4.3 for , $\Omega = 10$ and $\Omega = 15$, respectively. Figure 4.3 yields results similar to Figure 11.3 of reference [4] . Comparisons were made for the Fourier series solutions of magnetic frill generator as developed in [2] , and computer code generated in the course of this work and similar satisfactory results were observed . Hence the series solutions obtained numerically using such codes were used as reference solutions for subsequent comparisons of results based on varies frequency expansions developed in this work .

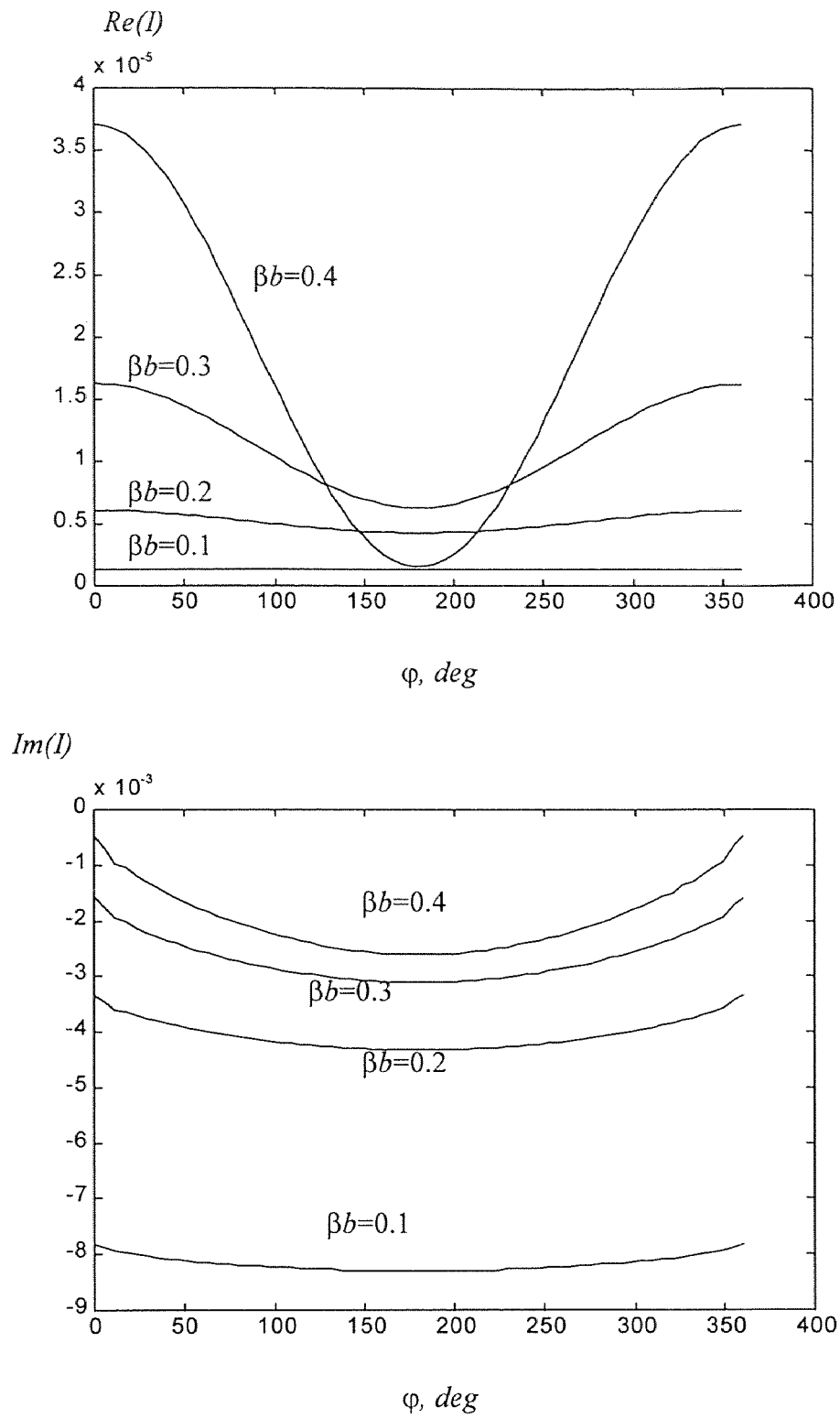


Fig. 4.1 Real and imaginary components of the normalized current in a delta-gap excited circular loop antenna, $\Omega=10$.

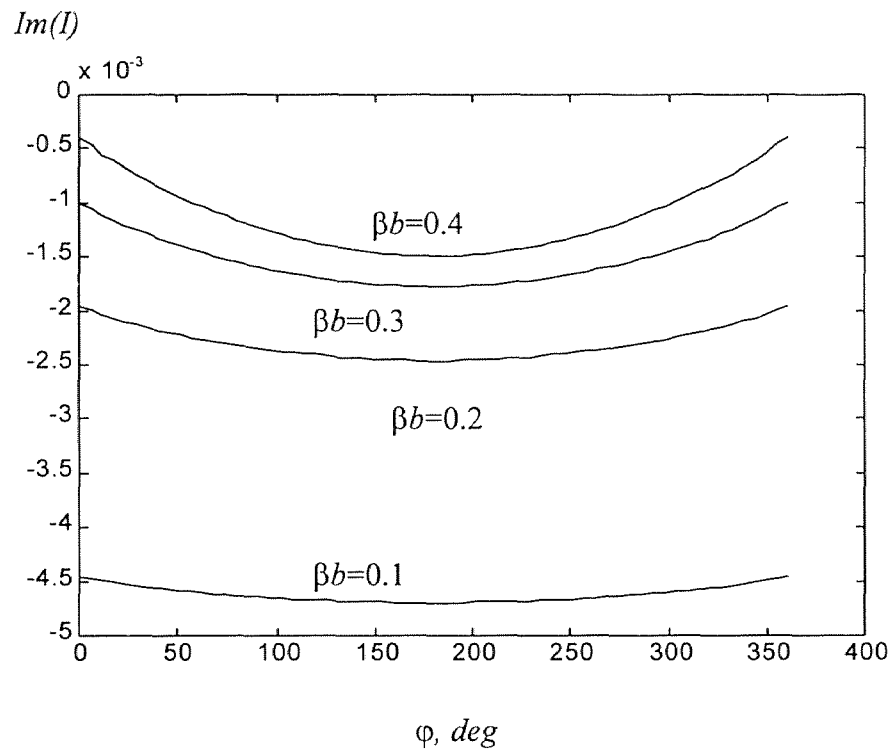
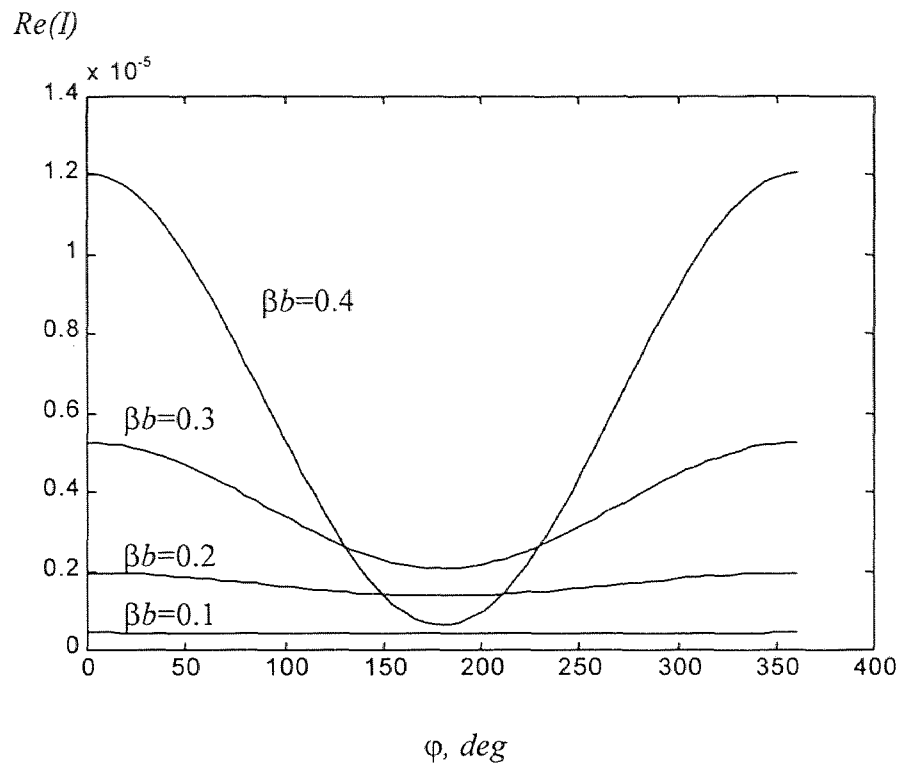


Fig. 4.2 Real and imaginary components of the normalized current in a delta-gap excited circular loop antenna, $\Omega=15$

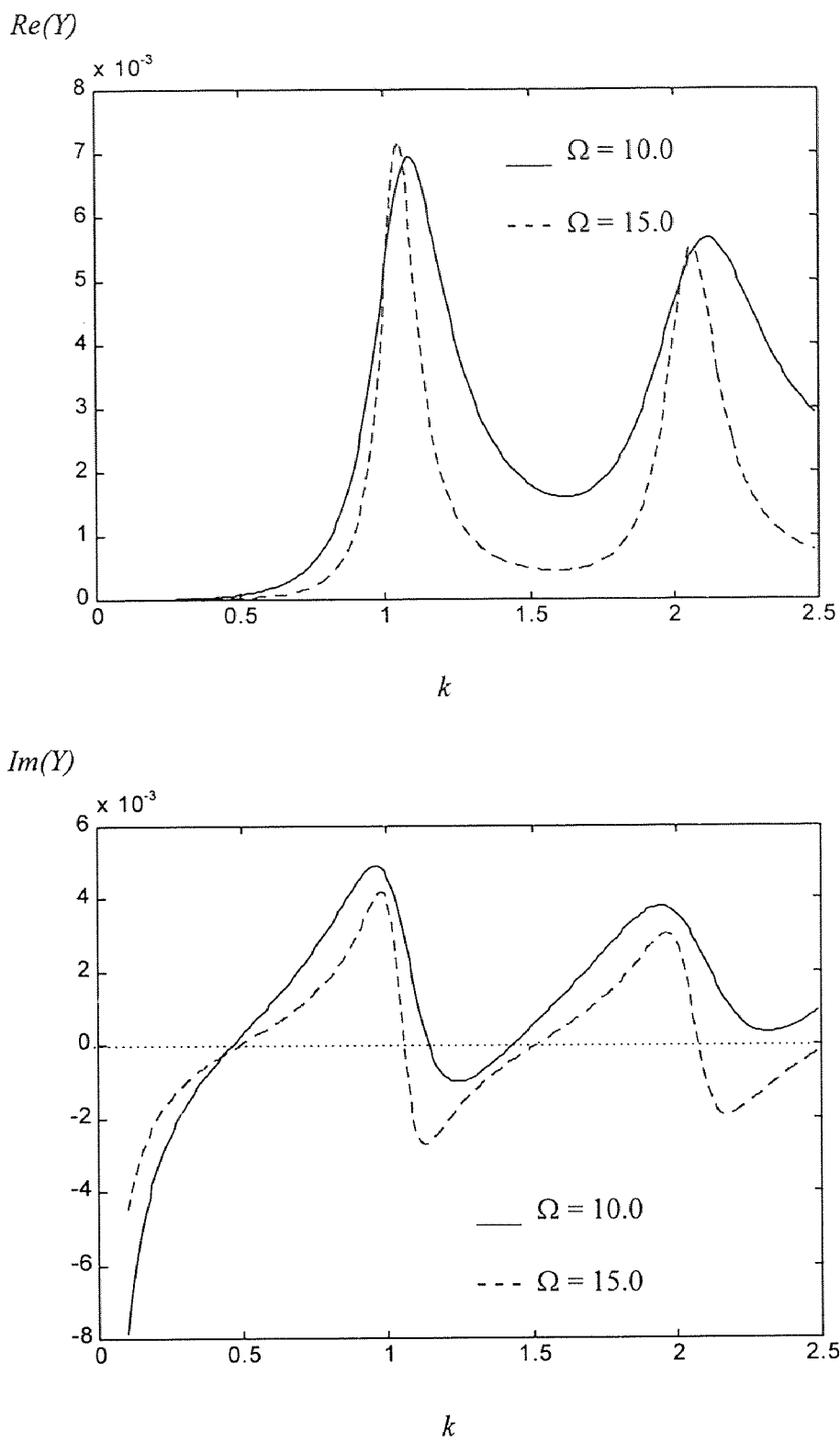


Fig. 4.3 Normalized Admittance with the Delta-Gap Excitation

The low frequency expansion in (2.45) around $k_0=0$ depicted in Figure 4.4 for the real part of the admittance agrees very well in the $0 < k < 0.05$ range whereas the imaginary part starts to deviate quite rapidly away from the expansion. This is very obvious due to divergent nature of susceptance around $k_0=0$ and more careful observation of Figure 4.4 results show that based on approximation predict the presence of a resonance ($\text{Im}\{Y\} = 0$) whereas the reference solution exhibits no sign of such resonance condition at these low frequencies. Further expansions around $k_0=0.1, 0.2$ and 0.3 exhibit similar behavior except that now deviations are much less in the region $\Delta k=0.1$ compared to $k_0=0$, as seen in Figure 4.5, 4.6, 4.7, respectively. Expansions around $k_0=0.4$ and $k_0=0.5$ exhibit excellent agreement with the reference solutions of Fourier series solutions as seen in Figure 4.8, 4.9, respectively.

Since the behavior around the resonance doesn't show rapid variations in the input susceptance, the four term expansion is adequate to lower the bandwidth $\Delta k=0.1$. Taylor's series expansion around $k = k_0$ is expected to produce a perfect match at the expansion point, and diverging behavior as observations are made further away from the expansion point. However, such behavior was not observed in most of the numerical results, shown in Figure 4.6 to 4.10 due to various approximations made in evaluation to avoid two dimensional numerical integration. The expansion coefficients in (2.45 - 2.46) are tabulated for various expansion points in Table 1, covering the frequency band $0 < k < 0.7$. Note that when the input admittance is to be determined, each coefficient has to be multiplied by the proper k dependence.

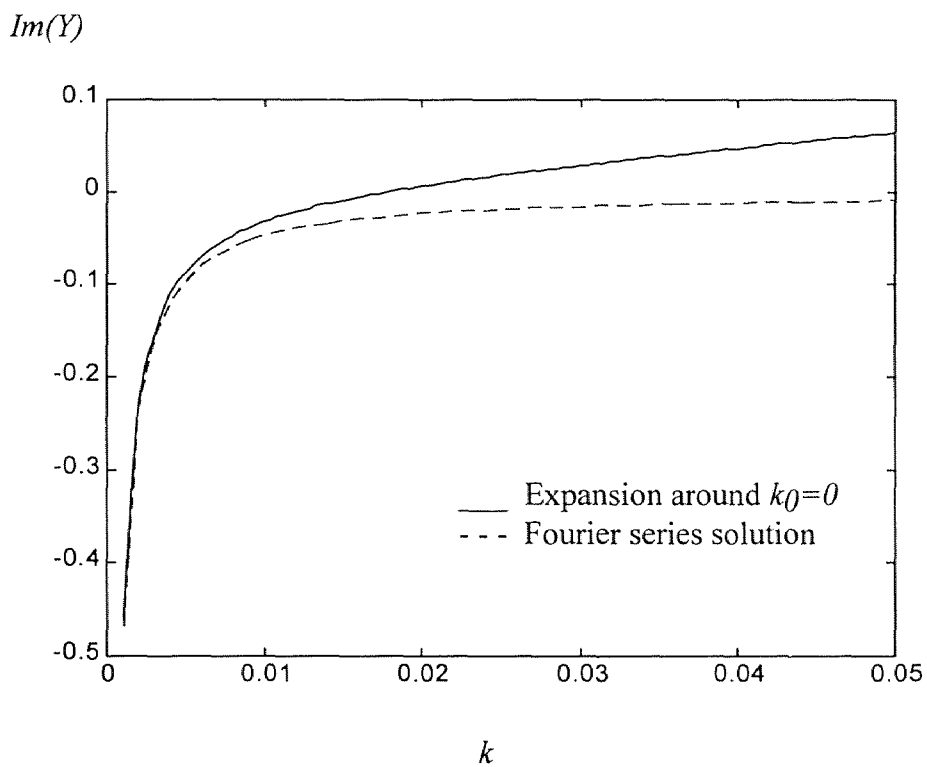
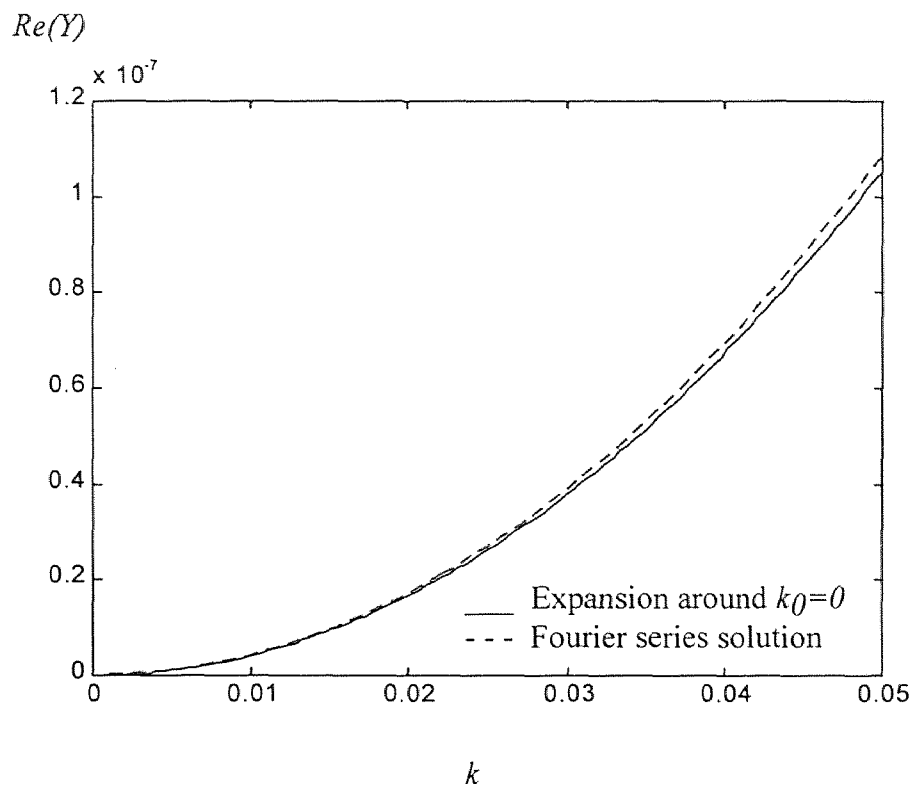


Fig. 4.4 Comparison of the delta-gap excited antenna input admittance calculated around $k_0 = 0$, versus Fourier Series Solution

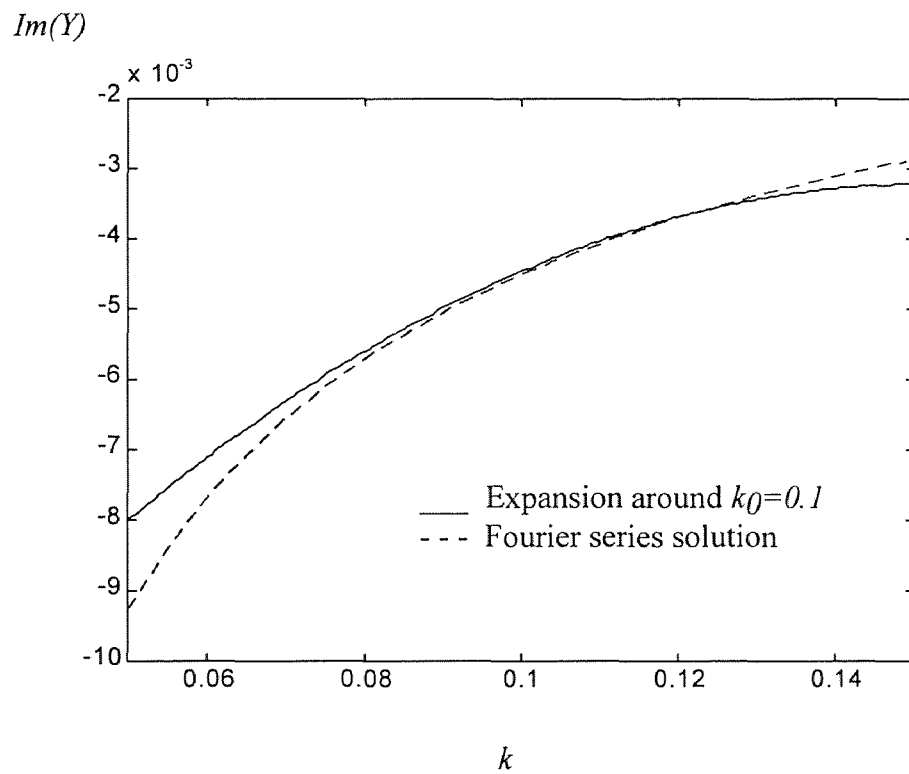
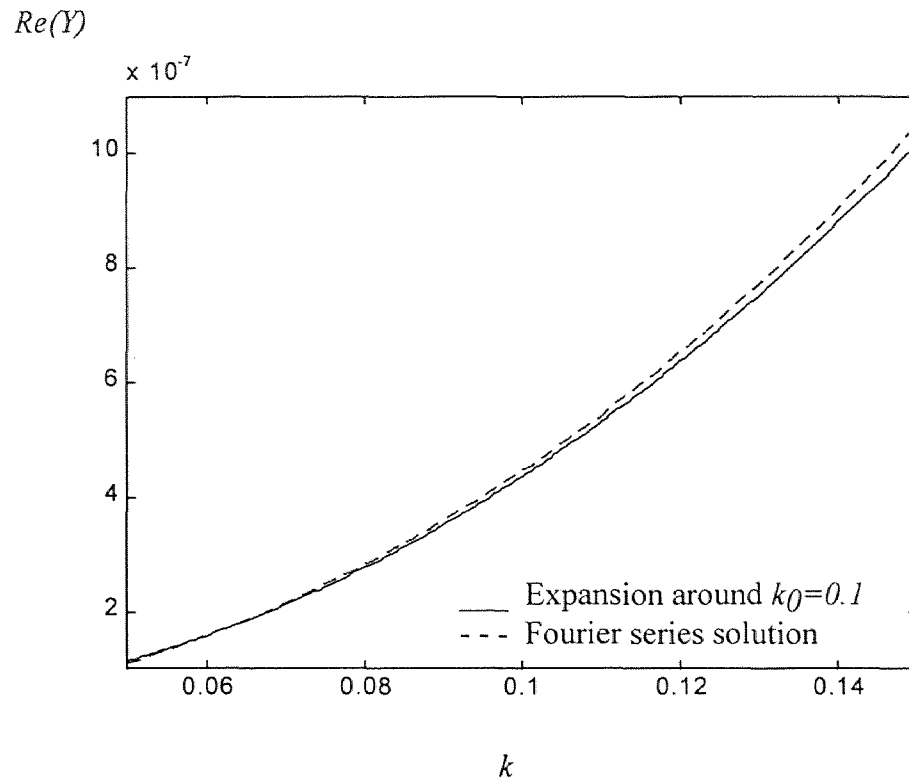


Fig. 4.5 Comparison of the delta-gap excited antenna input admittance calculated around $k_0=0.1$, versus Fourier Series Solution

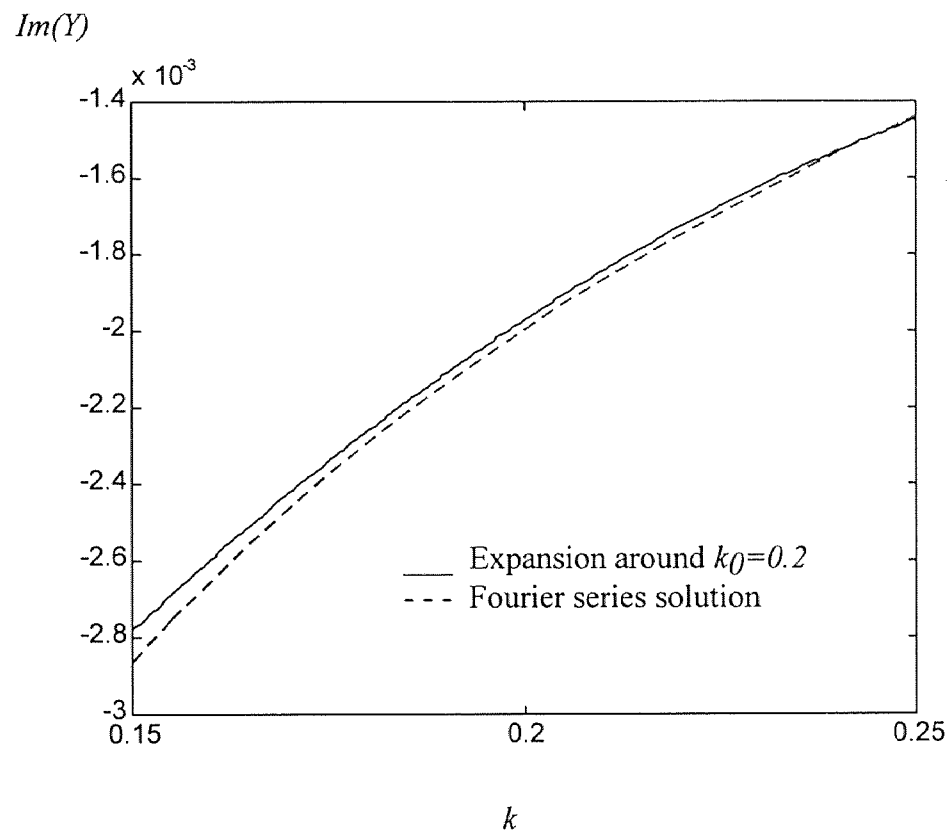
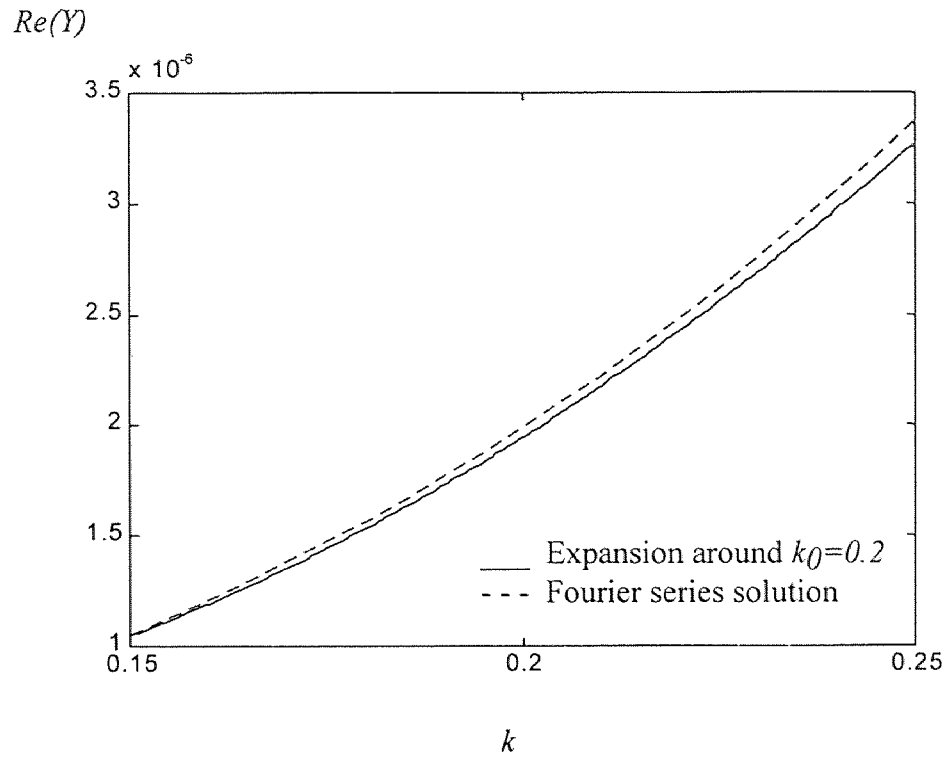


Fig. 4.6 Comparison of the delta-gap excited antenna input admittance calculated around $k_0=0.2$, versus Fourier Series Solution

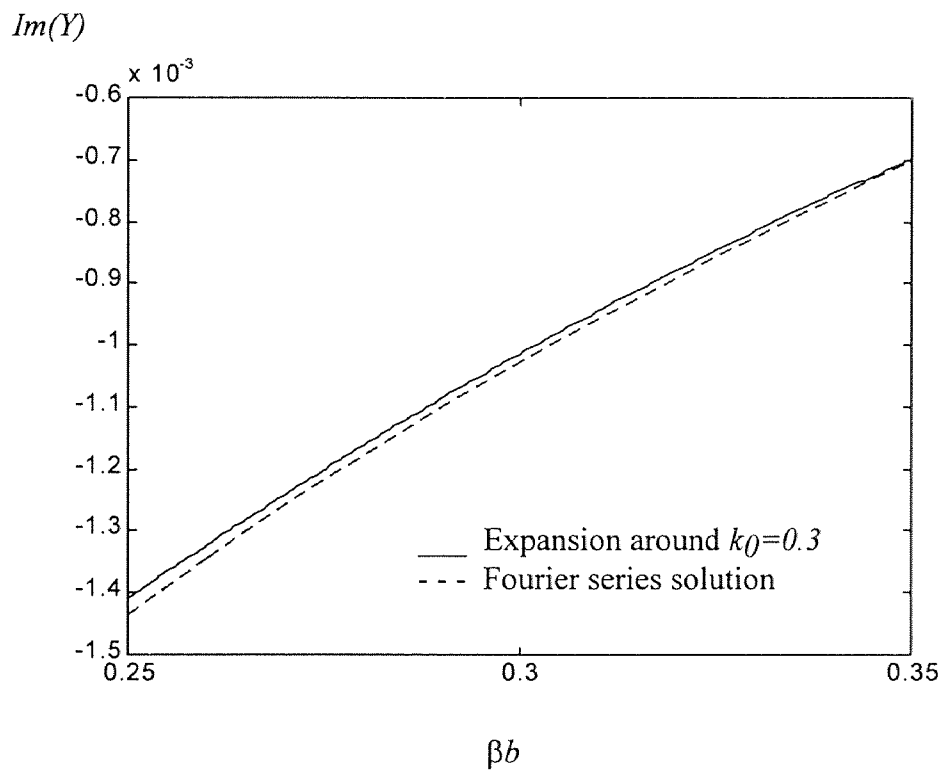
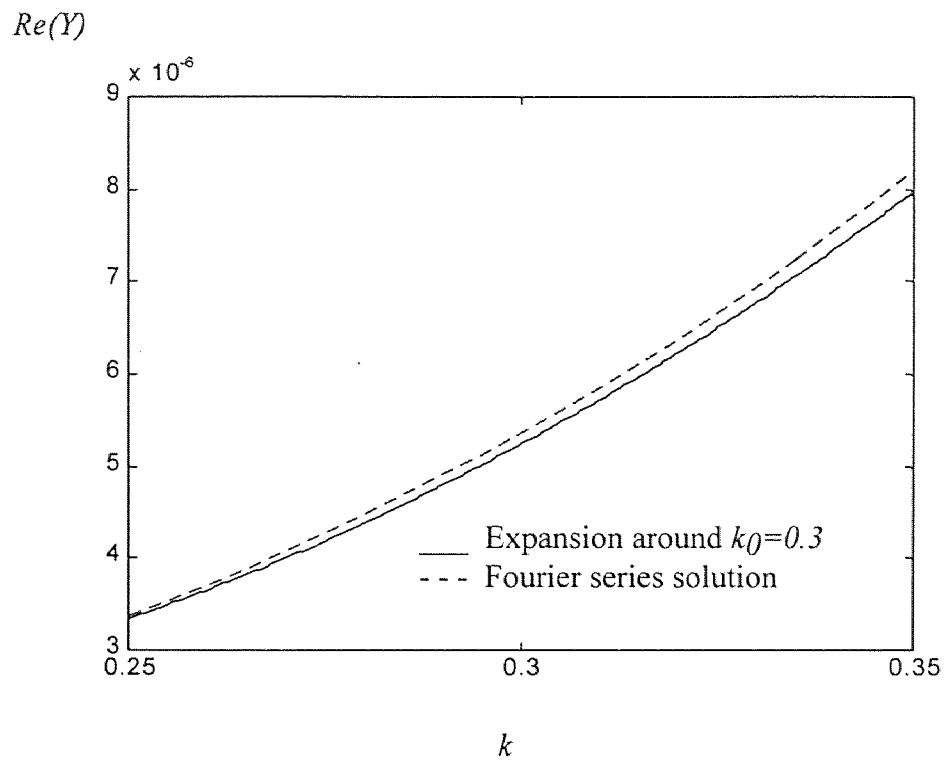


Fig. 4.7 Comparison of the delta-gap excited antenna input admittance calculated around $k_0=0.3$, versus Fourier Series Solution

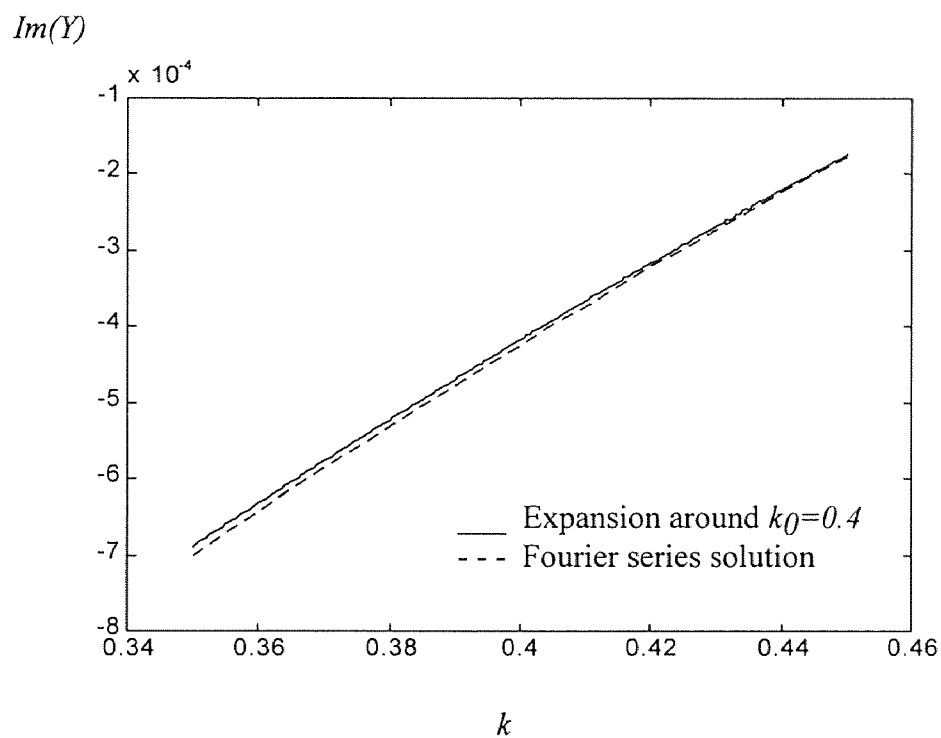
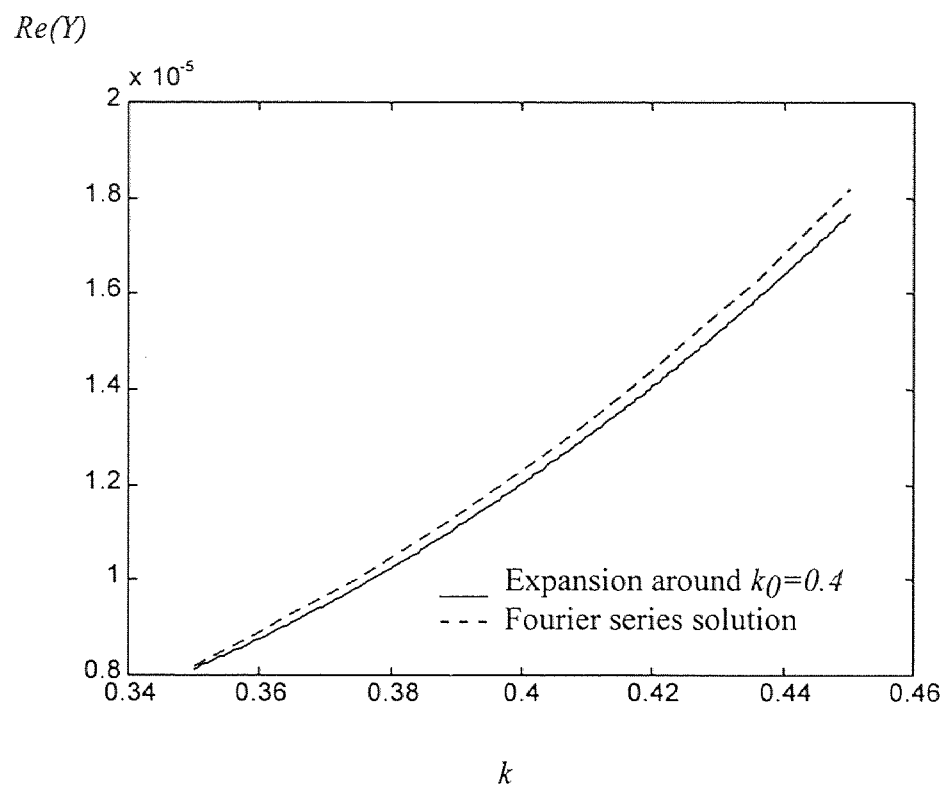


Fig. 4.8 Comparison of the delta-gap excited antenna input admittance calculated around $k_0=0.4$, versus Fourier Series Solution

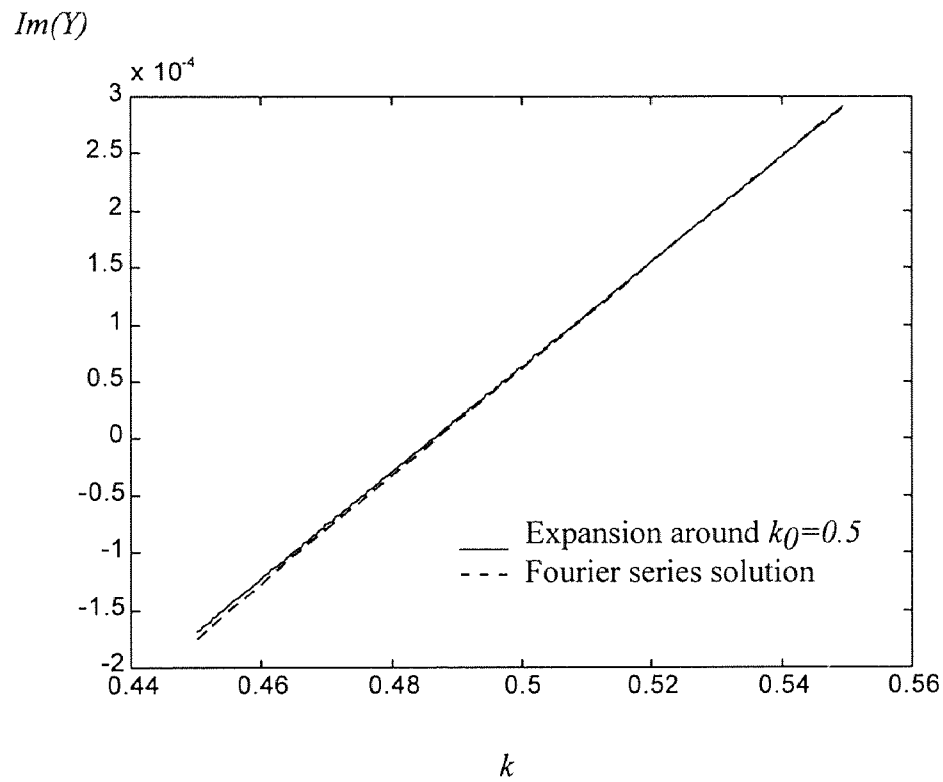
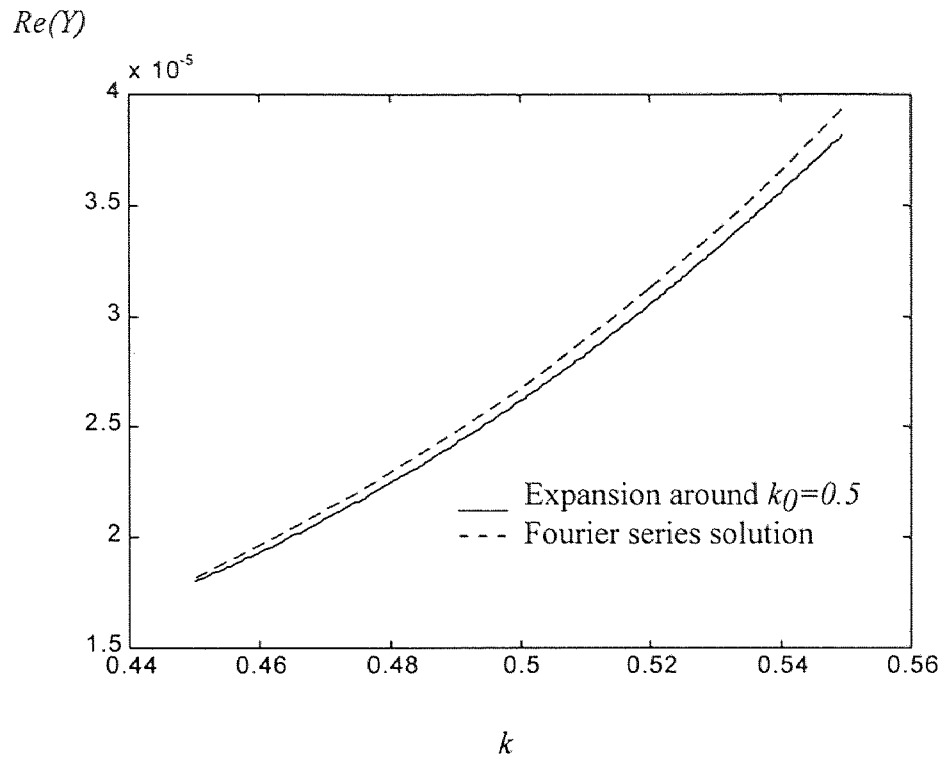


Fig. 4.9 Comparison of the delta-gap excited antenna input admittance calculated around $k_0=0.5$, versus Fourier Series Solution

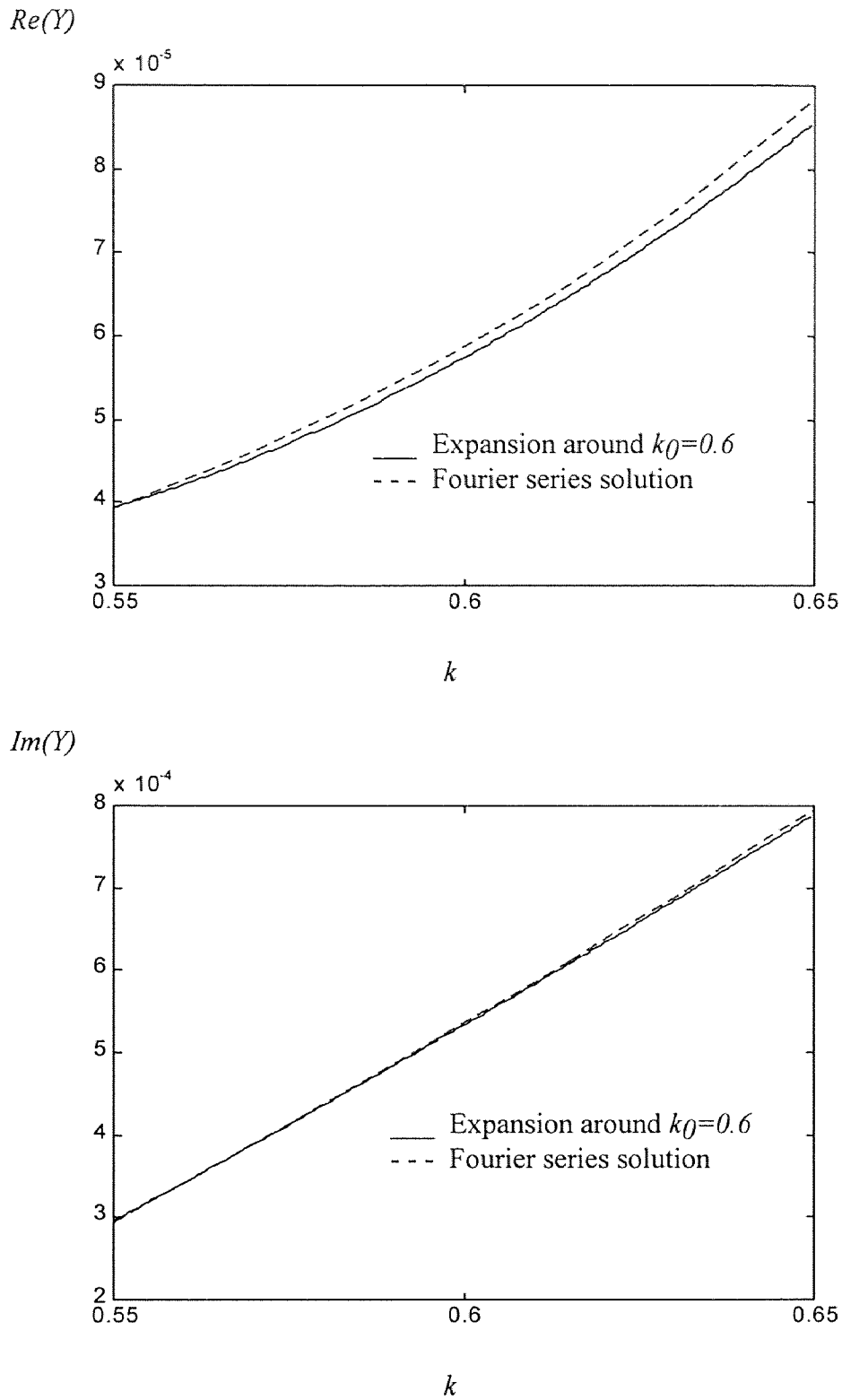


Fig. 4.10 Comparison of the delta-gap excited antenna input admittance calculated around $k_0 = 0.6$, versus Fourier Series Solution

Table 1. Expansion Coefficients for Input Admittance of delta-gap excited loop antenna

k_0	Y_{-1}	Y_0	Y_1	Y_2
0	$-j462.4e-06$	0	$j1.4703$	$42.166e-06$ $-j39.165e-06$
0.1	0	$47.99e-09$ $-j13.86e-03$	$-1.2725e-06$ $j140.34e-03$	$51.545e-06$ $-j462.04e-03$
0.2	0	$9.21e-09$ $-j6.925e-03$	$-12.007e-06$ $j36.201e-03$	$85.599e-06$ $-j57.134e-03$
0.3	0	$6.269e-06$ $-j4.582e-03$	$-53.167e-06$ $j16.687e-03$	$165.806e-06$ $-j15.973e-03$
0.4	0	$29.744e-06$ $-j3.329e-03$	$-184.12e-06$ $j9.404e-03$	$349.239e-06$ $-j5.3099e-03$
0.5	0	$123.37e-06$ $-j2.360e-03$	$-591.83e-06$ $j5.076e-03$	$794.638e-06$ $-j457.82e-06$
0.6	0	$503.772e-06$ $-j1.096e-03$	$-1.949e-03$ $j504.83e-06$	$2.089e-03$ $j3.687e-03$

The frill generator used in the source model of the loop antenna is expected to produce more accurate representation of the input susceptance. However, it is very difficult to carry out a one-to-one comparison due to mismatch in the physical dimensions of a delta-gap and the coaxial feed used in the magnetic frill excitation. The Fourier series solution of the magnetic frill excitation is chosen as a reference solution for frequency expansion developed in this work. Current distribution of Figure 4.11 and 4.12 and admittance variation of Figure 4.13 show very good agreement with the published results [2].

It is worthwhile to mention that the magnetic frill excitation yields much more accurate results when comparisons are made with experimental measurements. Comparison of various frequency expansions in the $0 < k < 0.7$ range showed very good agreement with the reference solutions which permit to construct equivalent circuit models of the loop antennas. Using expansion coefficients of Table 2 (or Table 1) the input admittance of the loop antenna can be expressed as

$$Y = Y_{-1} k^{-1} + Y_0 + Y_1 k + Y_2 k^2 \quad (4.14)$$

It is required to include additional terms to accommodate better physical interpretation of (4.14). It is reported [1] that in low frequency characterization of the loop antenna the real

part of the impedance $\text{Re}\{Z_m\} \cong \frac{\zeta \pi b^2 h^4}{6\pi}$. Presence of more terms will show that higher

order terms will be insignificant at lower frequencies due to the representation developed in this work.

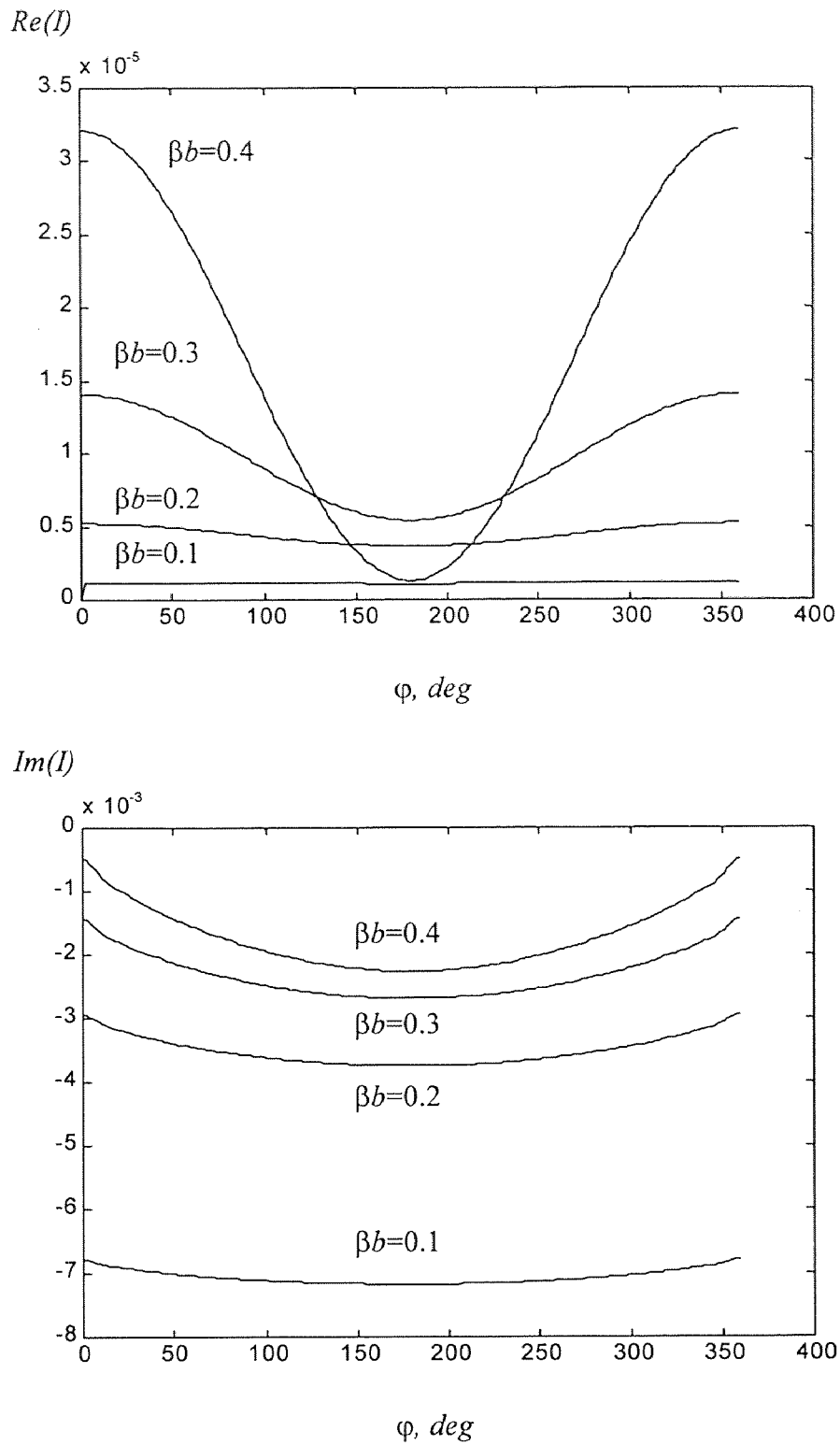


Fig. 4.11 Real and imaginary components of the normalized current in a frill excited loop antenna, $\Omega=10$. $a_0=a_i/0.24$

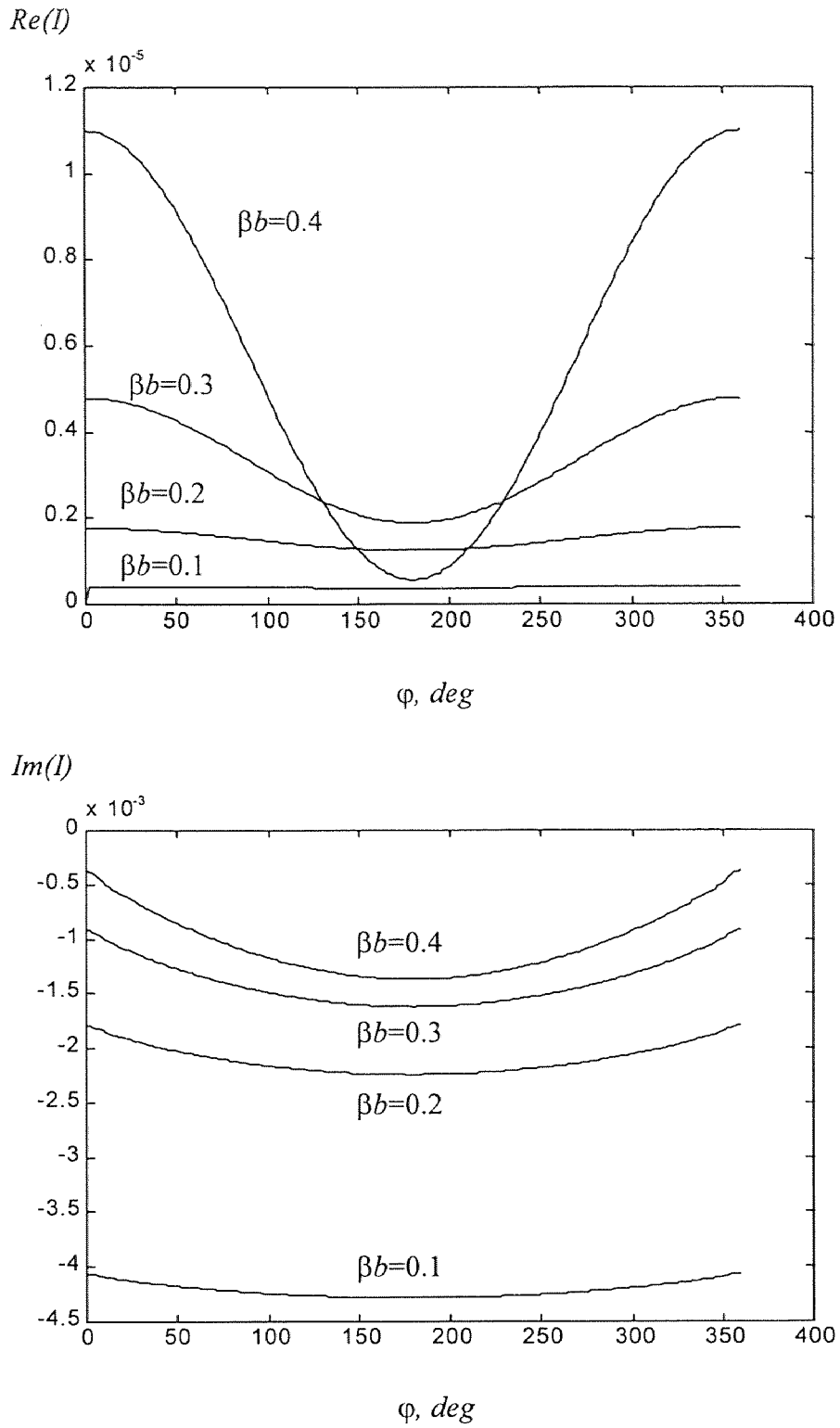


Fig. 4.12 Real and imaginary components of the normalized current in a frill excited loop antenna, $\Omega=15$, $a_o=a_i/0.24$.

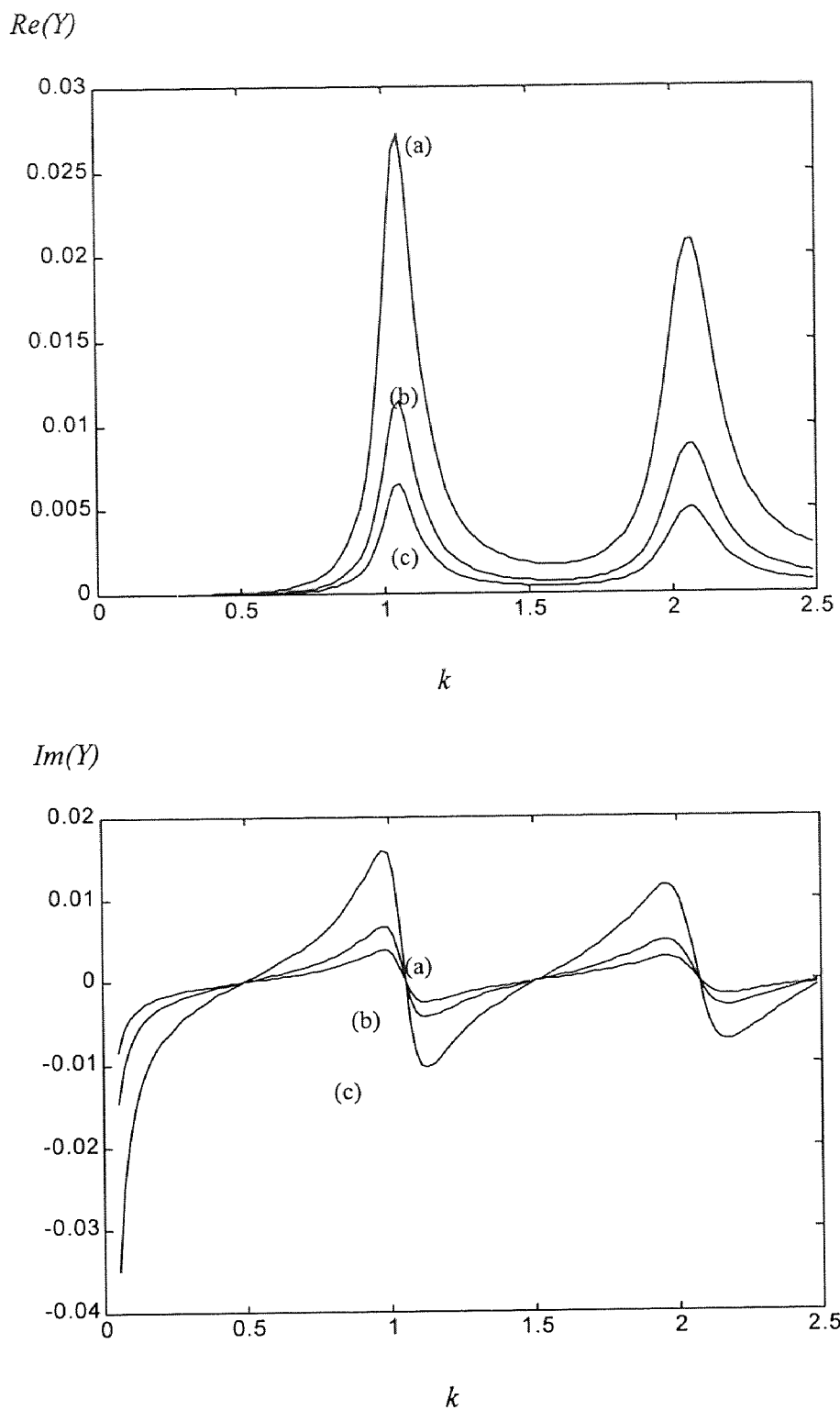


Fig. 4.13 Normalized Admittance with the Frill Excitation with $\Omega=15$
 (a) $a_o=a_i/0.24$ (b) $a_o=a_i/0.46$ (c) $a_o=a_i/0.74$

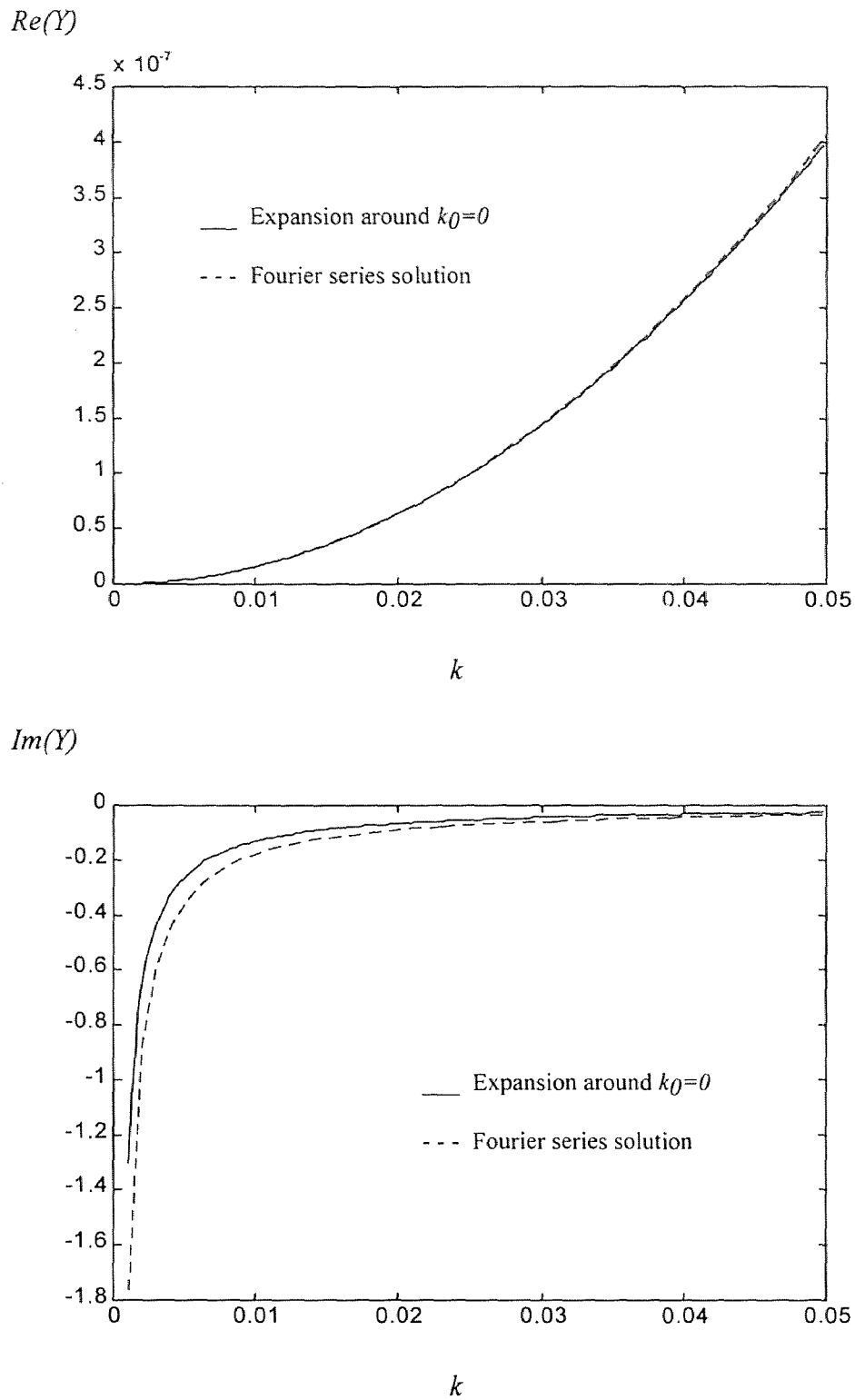


Fig. 4.14 Comparison of the frill excited antenna input admittance calculated around $k_0=0$, versus Fourier Series Solution

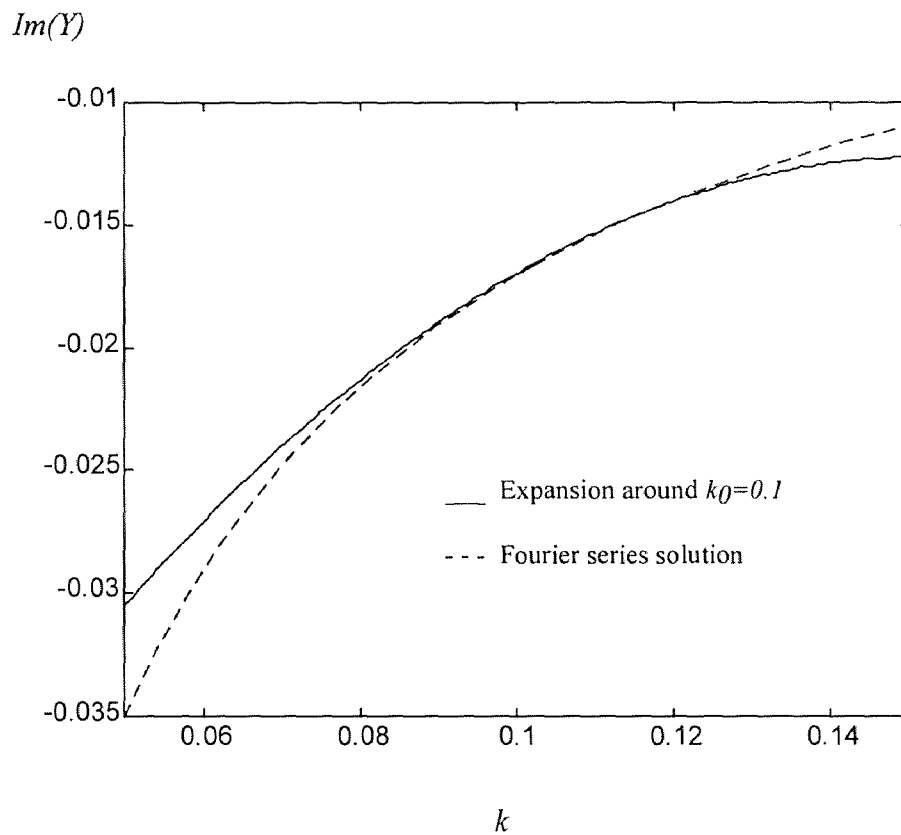
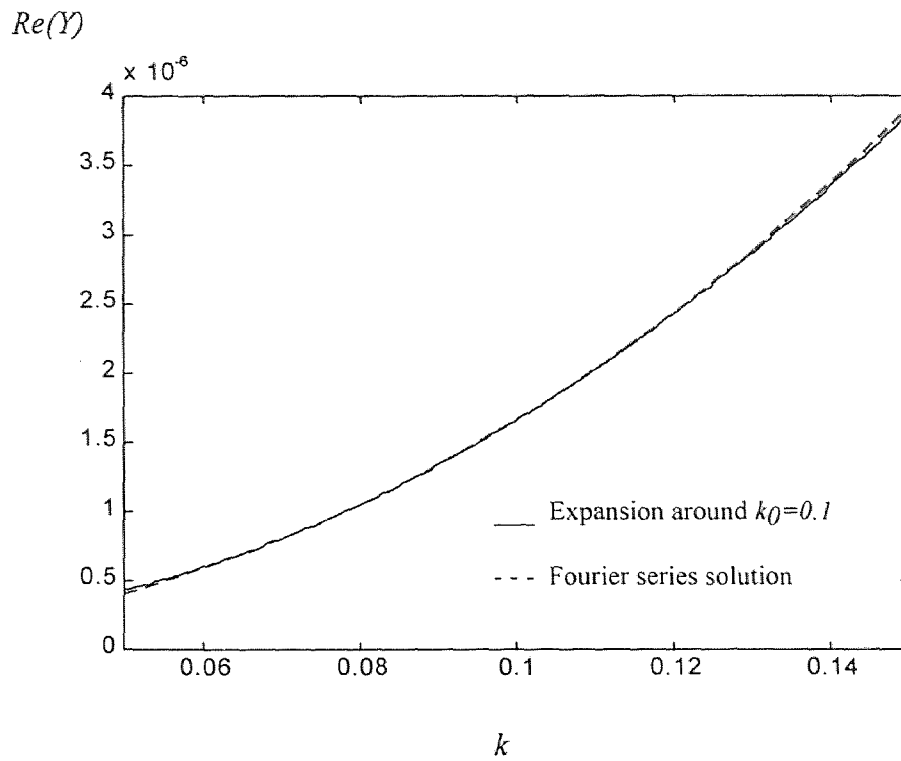


Fig. 4.15 Comparison of the frill excited antenna input admittance calculated around $k_0=0.1$, versus Fourier Series Solution

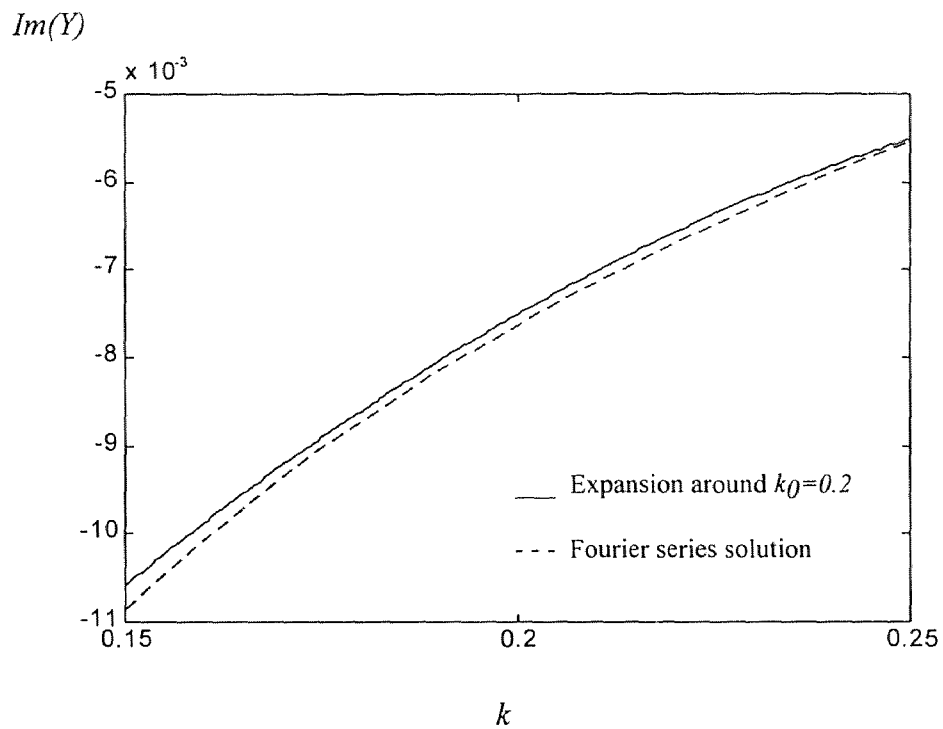
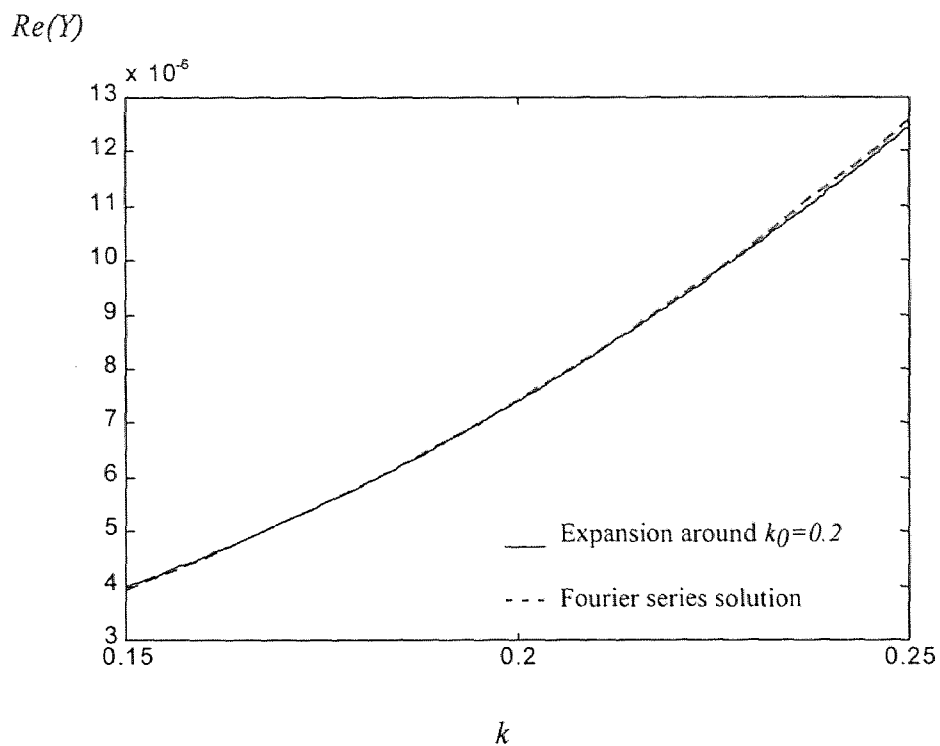


Fig. 4.16 Comparison of the frill excited antenna input admittance calculated around $k_0=0.2$, versus Fourier Series Solution

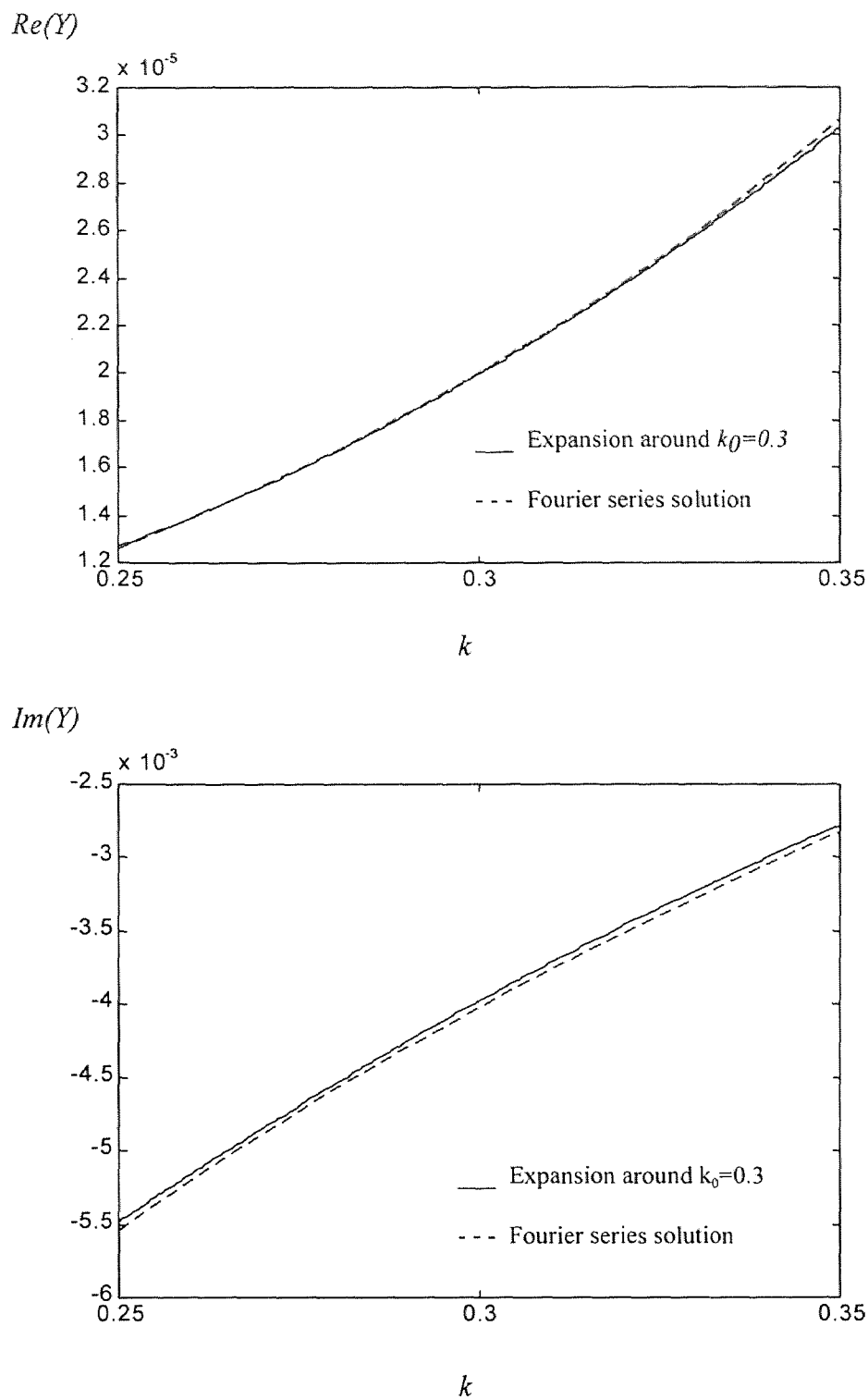


Fig. 4.17 Comparison of the frill excited antenna input admittance calculated around $k_0=0.3$, versus Fourier Series Solution

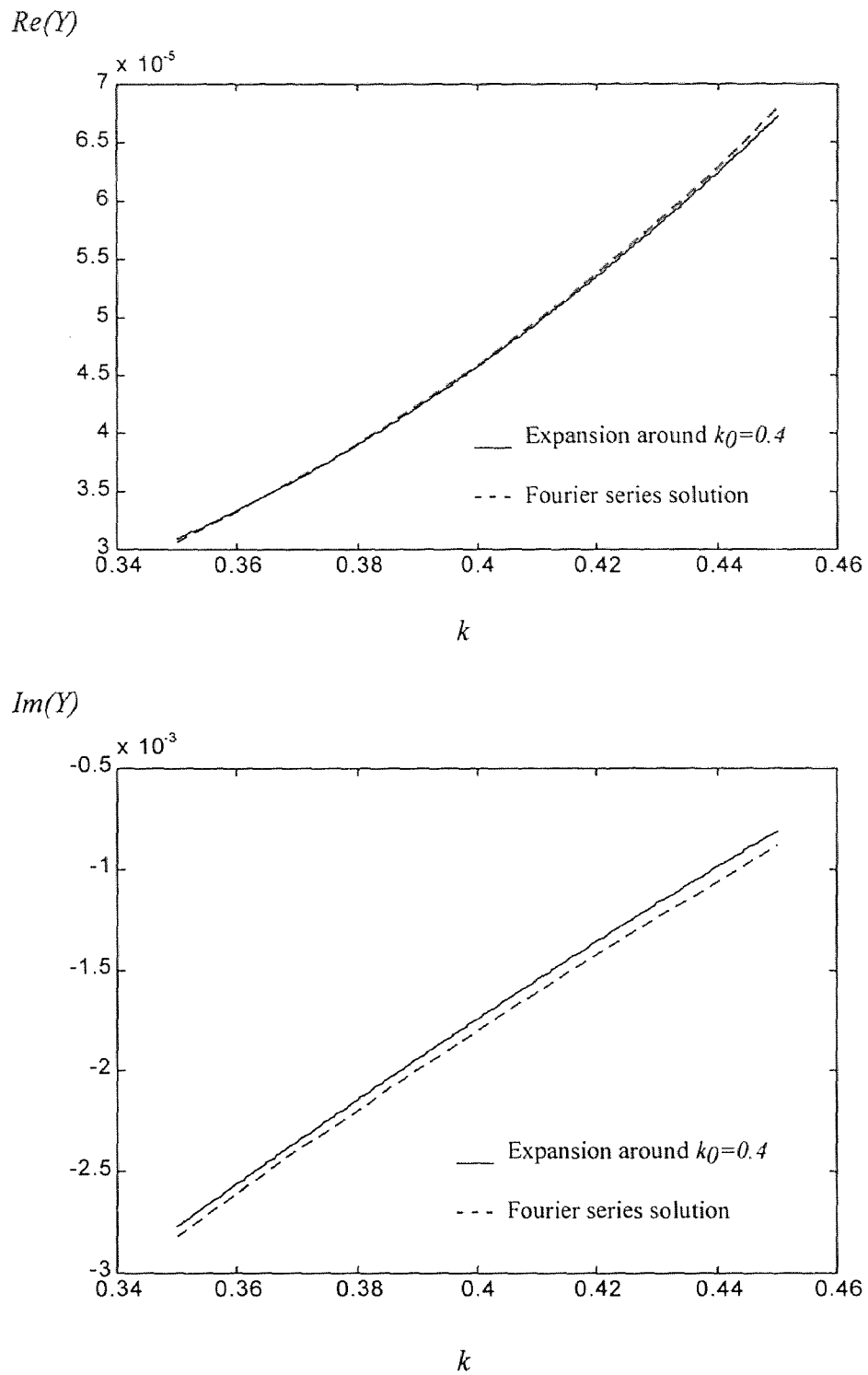


Fig. 4.18 Comparison of the frill excited antenna input admittance calculated around $k_0=0.4$, versus Fourier Series Solution

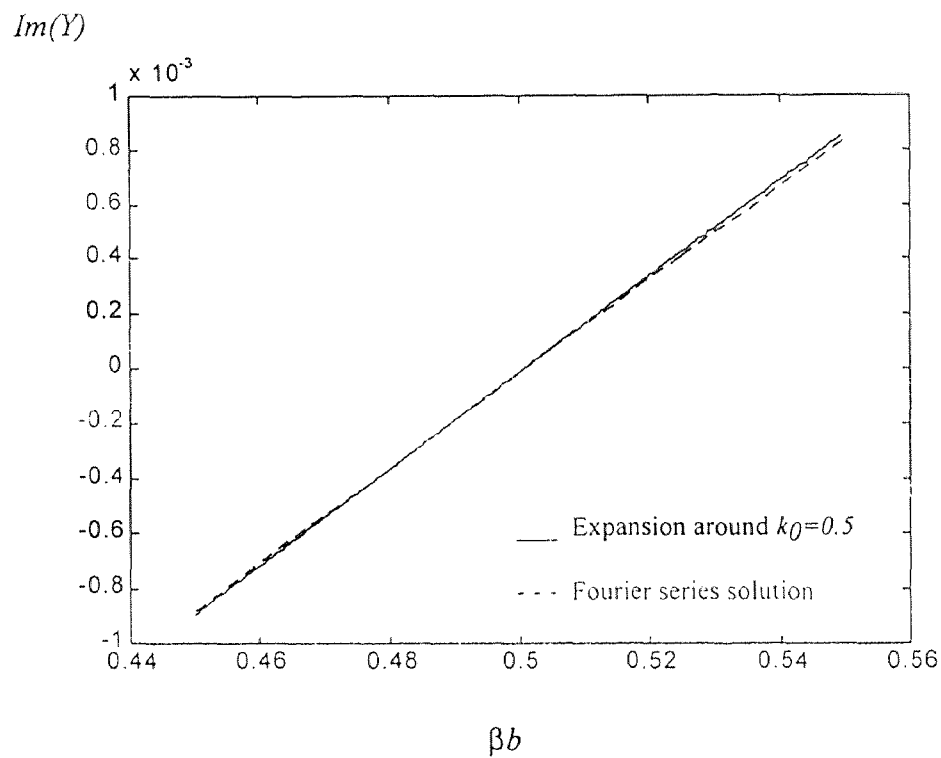
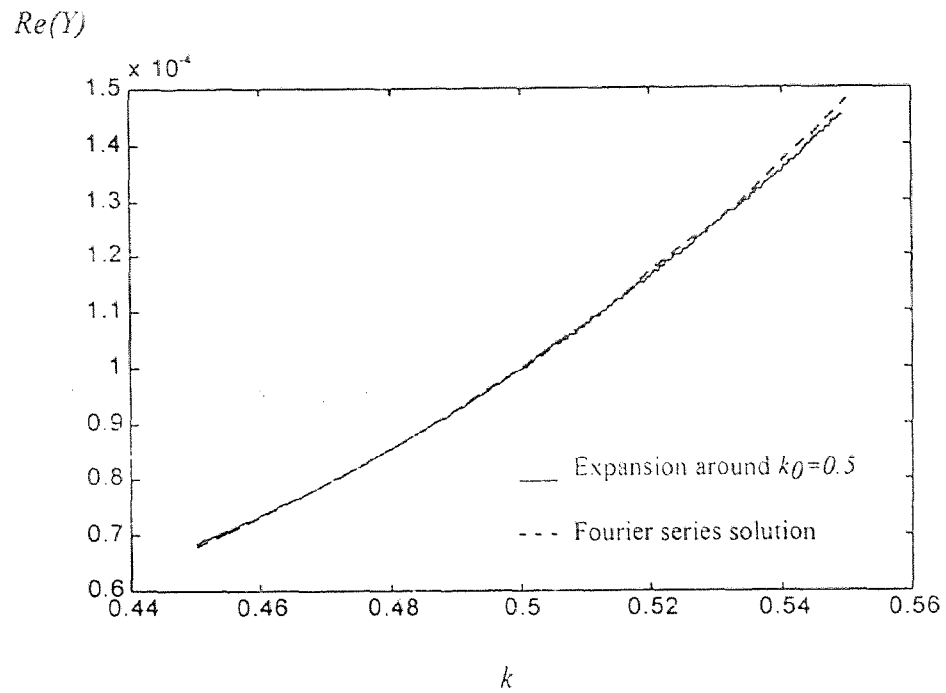


Fig. 4.19 Comparison of the frill excited antenna input admittance calculated around $k_0=0.5$, versus Fourier Series Solution

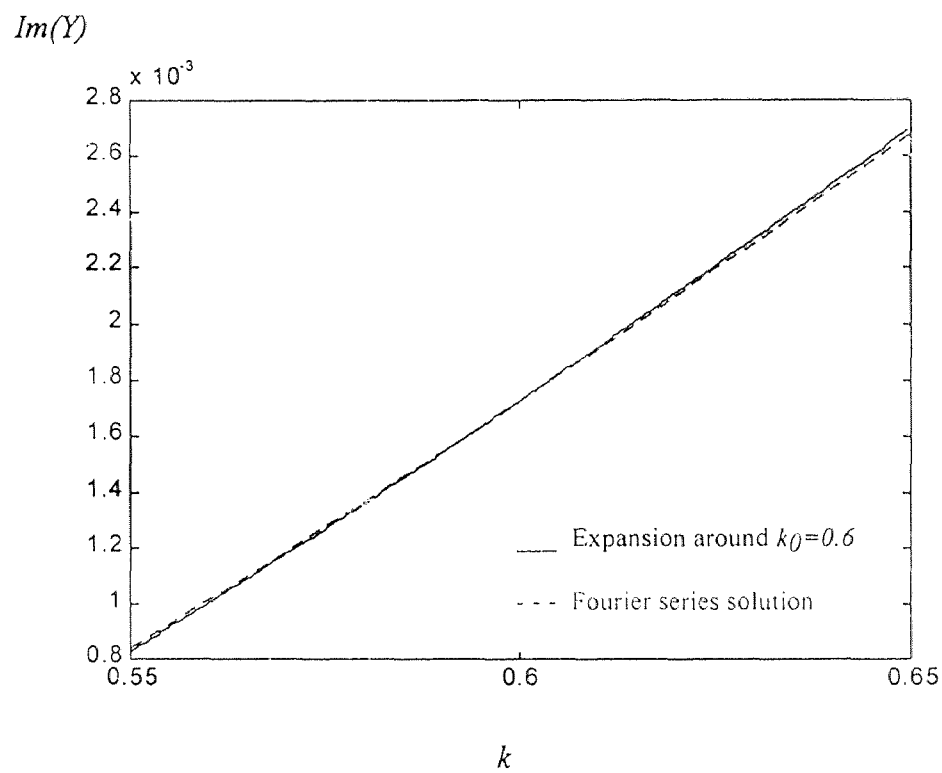
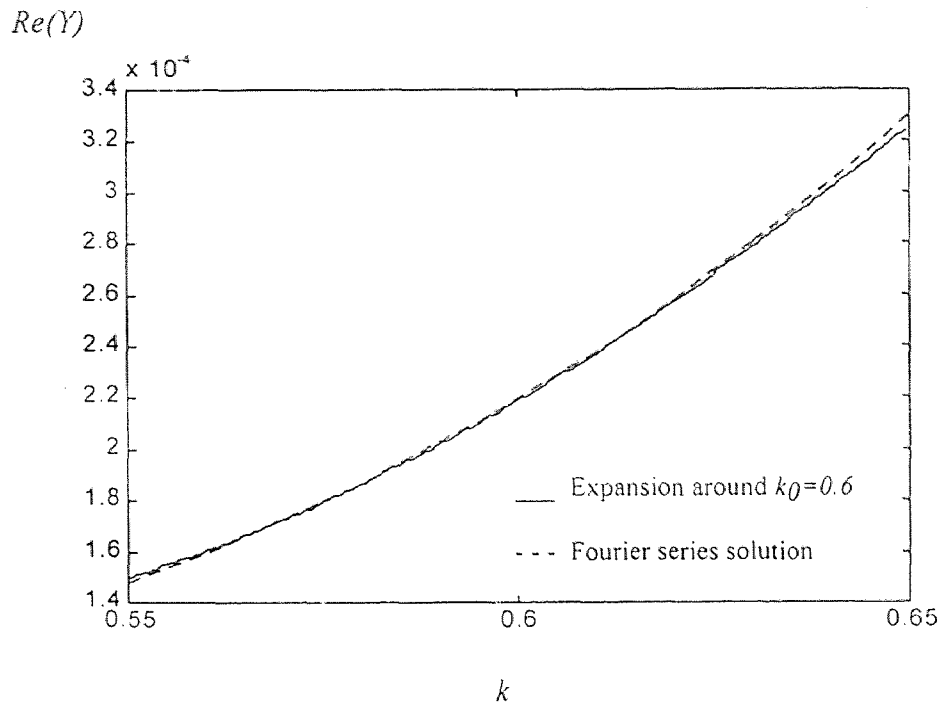


Fig. 4.20 Comparison of the frill excited antenna input admittance calculated around $k_0=0.6$, versus Fourier Series Solution

Table 2. Expansion Coefficients for the Admittance of the frill excited loop antenna

k_0	Y_{-1}	Y_0	Y_1	Y_2
0	$-j1.30516e-03$	0	$j3.267e-03$	$160.48e-06$
0.1	0	$182.52e-09$ $-j52.789e-03$	$-4.842e-06$ $j534.15e-03$	$196.46e-06$ $-j845.0e-06$
0.2	0	$3.507e-06$ $-j26.36e-03$	$-46.36e-06$ $j137.77e-03$	$325.32e-06$ $-j217.46e-03$
0.3	0	$23.86e-06$ $-j17.44e-03$	$-202.29e-06$ $j63.51e-03$	$631.10e-06$ $-j60.79e-03$
0.4	0	$113.31e-06$ $-j9.293e-03$	$-700.50e-06$ $j35.79e-03$	$1.329e-03$ $-j20.20e-03$
0.5	0	$469.82e-06$ $-j8.984e-03$	$-2.2526e-03$ $j19.3186e-03$	$3.025e-03$ $-j1.742e-03$
0.6	0	$1.917e-06$ $-j4.173e-03$	$-7.421e-03$ $j1.918e-03$	$7.649e-03$ $-j14.03e-03$

CHAPTER 5

CONCLUSIONS

The systematic low frequency expansions for the input admittance of the loop antenna have been developed. Computer codes have been generated to solve integral equation for the loop antenna with delta-gap and magnetic frill current feeds in terms of Fourier series. Results obtained using these codes served as a reference solution to compare various expansion models developed in this thesis. This formulation lead to the input admittance in the form of

$$Y = Y_{-1} k^{-1} + Y_0 + Y_1 k + Y_2 k^2$$

Such expansion yield very accurate models if the magnetic frill current is used, when comparison is made with experiment [2]. Another major advantage of limiting such an expansion to only few terms is the capability to identify each term with their corresponding inductance, conductance, capacitance, radiation admittance, etc.

Inclusion of few more terms is currently under investigation to identify more accurately the frequency dependence of these physical parameters of the loop antenna.

REFERENCES

- [1] R. W. P. King and C. W. Harrison, Jr., *Antenna and Waves: A Modern Approach*. Ch. 9, MIT Press, Cambridge, MA; 1969.
- [2] G. Zhou and G. S. Smith, "An Accurate Theoretical Model for the Thin-Wire Circular Half-Loop Antenna." *IEEE Trans. Antennas Propagat.*, vol. 39, pp. 1167-1177, May 1991.
- [3] E. Niver, H. Smith and G. Whitman, "Frequency Characterization of a Thin Linear Antenna Using Diakoptic Antenna Theory." *IEEE Trans. Antennas Propagat.*, vol.40, pp. 245-250, Aug. 1992.
- [4] R. E. Collin and F. J. Zucker, *Antenna Theory. Part 1*. Ch. 11, McGraw-Hill, 1969.
- [5] J. A. Stratton, *Electromagnetic Theory*. McGraw-Hill, New York, 1941